

AD/A-005 662

STRENGTH, DEFORMATION AND FRICTION
OF IN SITU ROCK

H. R. Pratt, et al

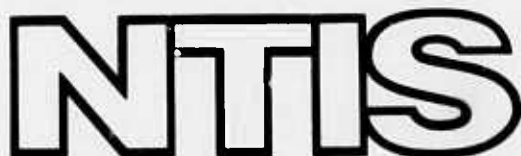
Terra Tek, Incorporated

Prepared for:

Air Force Weapons Laboratory
Advanced Research Projects Agency

December 1974

DISTRIBUTED BY:



National Technical Information Service
U. S. DEPARTMENT OF COMMERCE

066234

AD A 005662



STRENGTH, DEFORMATION AND FRICTION OF IN SITU ROCK

H. R. Pratt
A. D. Black
Terra Tek, Inc.
Salt Lake City, UT 84108

December 1974

Final Report for Period November 1972 - December 1973

Approved for public release; distribution unlimited.

Reproduced by
NATIONAL TECHNICAL
INFORMATION SERVICE
U.S. Department of Commerce
Springfield, VA 22151

Prepared for
ADVANCED RESEARCH PROJECTS AGENCY
1400 Wilson Blvd
Arlington, VA 22209

AIR FORCE WEAPONS LABORATORY
Air Force Systems Command
Kirtland Air Force Base, NM 87117

D D C
REFINED
FEB 18 1975
D
RECORDED
D

This final report was prepared by the Terra Tek, Inc., Salt Lake City, Utah, under Contract F29601-72-C-0121, Job Order 15151401, with the Air Force Weapons Laboratory, Kirtland AF, New Mexico. Major George V. Bulin (DEV) was the Laboratory Project Officer-in-Charge.

When US Government drawings, specifications, or other data are used for any purpose other than a definitely related Government procurement operation, the Government thereby incurs no responsibility nor any obligation whatsoever, and the fact that the Government may have formulated, furnished, or in any way supplied the said drawings, specifications, or other data is not to be regarded by implication or otherwise as in any manner licensing the holder or any other person or corporation or conveying any rights or permission to manufacture, use, or sell any patented invention that may in any way be related thereto.

This technical report has been reviewed and is approved for publication.

G V Bulin Jr
GEORGE V. BULIN, JR.
Major, USAF
Project Officer

FOR THE COMMANDER

John J. Osborn
JOHN J. OSBORN
Lt Colonel, USAF
Chief, Facility Survivability
Branch

William B. Liddicoet
WILLIAM B. LIDDICOET
Colonel, USAF
Chief, Civil Engineering Research
Division

ACCESSION IN	
RTIS	White Section <input checked="" type="checkbox"/>
DDC	Buff Section <input type="checkbox"/>
UNARMED	<input type="checkbox"/>
JUSTIFICATION	
BY	
DISTRIBUTION/AVAILABILITY CODES	
DIST.	AVAIL. and <input checked="" type="checkbox"/> SPECIAL
<i>A</i>	

DO NOT RETURN THIS COPY. RETAIN OR DESTROY.

UNCLASSIFIED

SECURITY CLASSIFICATION OF THIS PAGE (When Data Entered)

REPORT DOCUMENTATION PAGE			READ INSTRUCTIONS BEFORE COMPLETING FORM
1. REPORT NUMBER AFWL-TR-74-24	2. GOVT ACCESSION NO.	3. RECIPIENT'S CATALOG NUMBER AD/A005 662	
4. TITLE (and Subtitle) STRENGTH, DEFORMATION AND FRICTION OF IN SITU ROCK		5. TYPE OF REPORT & PERIOD COVERED Final Report; November 1972-December 1973	
7. AUTHOR(s) H. R. Pratt; A. D. Black		8. CONTRACT OR GRANT NUMBER(s) F29601-72-C-0121	
9. PERFORMING ORGANIZATION NAME AND ADDRESS Terra Tek, Inc. University Research Park Salt Lake City, UT 84108		10. PROGRAM ELEMENT, PROJECT, TASK AREA & WORK UNIT NUMBERS 62701D; 15151401; ARPA Order 1575, Amdt-2	
11. CONTROLLING OFFICE NAME AND ADDRESS Advanced Research Projects Agency Arlington, VA 22209		12. REPORT DATE December 1974	
14. MONITORING AGENCY NAME & ADDRESS (if different from Controlling Office) Air Force Weapons Laboratory (DEV) Kirtland AFB, NM 87117		15. SECURITY CLASS. (of this report) UNCLASSIFIED	
16. DISTRIBUTION STATEMENT (of this Report) Approved for public release; distribution u limited.		18. DECLASSIFICATION/DOWNGRADING SCHEDULE D D C DRAFTED FEB 18 1975 REFUGEE D	
17. DISTRIBUTION STATEMENT (of the abstract entered in Block 20, if different from Report)			
18. SUPPLEMENTARY NOTES			
19. KEY WORDS (Continue on reverse side if necessary and identify by block number) Rock properties; Material properties; Material testing; Rock mechanics; Rock dynamics; In situ testing; Rock fracture			
20. ABSTRACT (Continue on reverse side if necessary and identify by block number) A field and laboratory program was conducted at several test sites to determine the strength, deformation, and frictional properties of a variety of rock types (sandstone, amphibolite, quartz diorite). The test results at Auburn and Glen Canyon dams compared favorably with those obtained by the US Bureau of Reclamation. A series of in situ and laboratory specimens from the MIXED COMPANY site were tested to determine the effects of specimen size, saturation, and anisotropy on the strength and deformation of massive sandstone. Direct and proportional shear tests were conducted to determine the effect			

UNCLASSIFIED

SECURITY CLASSIFICATION OF THIS PAGE(When Data Entered)

of load path on frictional properties. The load paths in the laboratory tests simulated the paths followed during loading of in situ specimens. Load path was found to have an effect on the friction angle of natural joints. The shear stiffness was found to be a function of normal stress. Given accurate joint maps (orientation, frequency, and continuity) and measured frictional and deformation properties, it should be possible using size effect to predict the mechanical response of a jointed rock mass.

ia UNCLASSIFIED

SECURITY CLASSIFICATION OF THIS PAGE(When Data Entered)

PREFACE

The *in situ* tests were conducted at several damsites regulated by the U.S. Bureau of Reclamation. The assistance of the following personnel at the Bureau of Reclamation is gratefully acknowledged:

H. G. Arthur, Director, Design and Construction and M. H. Logan, Chief, Geology and Geotechnology Branch of the Engineering and Research Center, Denver; R. Rolin and L. Frei at the Auburn Dam; L. DeGuire, F. Carlson and G. Boyt at the Morrow Point Dam; and H. R. Gnau, C. Keller, H. Gilleland and L. K. Newhouse at Glen Canyon Dam. Discussions with W. F. Brace, W. Wawersik and H. Swolfs on frictional properties and test procedures were most beneficial.

This program was sponsored by the Advanced Research Project Agency, Dr. Stanley Rubey co-ordinator and monitored by Captain S. Chisolm and Major G. Bulin, Air Force Weapons Laboratory, United States Air Force, Kirtland Air Force Base, New Mexico. We thank Dr. Rubey, Captain Chisolm, Major Bulin and Mr. Jimmie Bratton (AFWL) for their encouragement and assistance. W. F. Brace, J. Bratton and G. Bulin critically read the manuscript. Terra Tek contribution 73-68.

TABLE OF CONTENTS

Section I. Introduction	1
Section II. Test Site Locations	3
Morrow Point Damsite	3
Mixed Company Test Site.	6
Auburn Damsite	8
Glen Canyon Dam.	11
Section III. Test Program	13
Field Program.	13
Laboratory Program	13
Section IV. Experimental Techniques	17
Specimen Preparation	17
Loading System	19
Instrumentation.	21
Section V. Test Procedure	24
<i>In Situ</i> Deformation Tests on Intact and Jointed Rock	24
Laboratory Tests	24
Section VI. Experimental Results.	26
Auburn Damsite	26
Mixed Company.	26
Size Effects	29
Anisotropy	29
Effect of Saturation	31
Effect of Porosity	31

Section VI. Experimental Results (continued)	
Glen Canyon.	34
Cedar City Test Site	39
Section VII. Discussion	55
Size Effects	60
Deformation and Strength	65
Section VIII. Conclusions	76
References	78

LIST OF FIGURES

<u>Figure No.</u>	<u>Description</u>	<u>Page</u>
1.	Highly foliated Precambrian schist and gneiss, Morrow Point dam, Colorado.	5
2.	Stratigraphic section at the Mixed Company test site.	7
3.	Test site location at the Mixed Company test site.	9
4.	Drill rig is positioned for slotting of <i>in situ</i> specimen at Mixed Company test site. CIST site and cores in background.	9
5.	Schematic of U.S. Bureau of Reclamation <i>in situ</i> direct shear test, Auburn damssite, California. (Ref.1)	10
6.	Instrumented <i>in situ</i> test in exploratory adit at Auburn damssite. Radial jacking test location (USBR) is seen at far right.	10
7.	Massive cross-bedded Navajo sandstone located at Glen Canyon, Arizona.	12
8.	Test site location in adit at Glen Canyon dam.	12
9.	Test location and drilling rig at Morrow Point dam, Colorado.	14
10.	Specimen of chloritic schist being excavated on vertical wall, Auburn dam, California.	14
11.	Drilling rig and partially prepared <i>in situ</i> specimen. Flatjack package at left.	18
12.	Special drilling frame developed for specimen preparation in the Auburn damssite exploratory adit.	18
13.	Schematic of the pneumatic-hydraulic pumping system.	20
14.	Schematic of instrumentation layout.	22
15.	Servo-controlled direct shear machine.	22
16.	Computer output from typical direct shear test.	23
17.	<i>In situ</i> stress-strain response of amphibolite and chloritic schist, Auburn damssite, California.	27

18.	Friction envelopes for amphibolite, Auburn damsite, California.	28
19.	Shear stress versus displacement for field and laboratory tests, Auburn, California.	28
20.	Effect of specimen size on strength for Kayenta sandstone, Mixed Company site, Colorado.	30
21.	Strength as a function of density for specimen cored perpendicular and parallel to bedding.	30
22.	Elastic modulus as a function of density for specimens cores perpendicular and parallel to bedding.	32
23.	Failure as a function of percent saturation.	33
24.	Photomicrograph of Kayenta sandstone (x 30).	35
25.	Stress difference as a function of density for triaxial tests up to $P_c = 4.0$ kbars.	35
26.	Shear stress-displacement for <i>in situ</i> and laboratory 45° proportional shear tests, Glen Canyon.	36
27.	Stress-strain results for intact <i>in situ</i> specimen, Glen Canyon.	36
28.	Relation of τ vs. σ_n for <i>in situ</i> and laboratory direct shear and 45° proportional shear tests, Glen Canyon.	38
29.	Comparison of τ vs. σ_n for laboratory specimen with natural joints and bedding planes, Glen Canyon.	38
30.	Typical profile of natural and artificial joints, Cedar City.	42
31.	Direct shear and proportional shear load paths.	42
32.	Field specimen joint orientation.	43
33.	Shear stress-normal stress curve for 45° proportional load path, Cedar City.	43
34.	Data scatter and statistical fit of τ vs σ_n curves for natural joints sheared under various load paths, Cedar City.	45
35.	Data scatter and statistical fit of τ vs σ_n curves for saw-cut joints sheared under various load paths, Cedar City.	45

36.	Data scatter and statistical fit of τ vs σ_n curves for Brazilian joints sheared under various load paths, Cedar City.	45
37.	Shear stress-displacement curves for natural joints (Cedar City) sheared at various normal stresses and 30° , 45° and direct shear load paths.	46
38.	Shear stress-displacement curves for saw-cut joints (Cedar City) sheared at various normal stresses and 30° , 45° and direct shear load paths.	46
39.	Shear stress-displacement for a saw-cut joint cycled at different normal stresses, Cedar City.	47
40.	Shear stress-displacement for a single virgin and repositioned natural joint, Cedar City.	49
41.	Shear stress-normal stress for a single, virgin and repositioned natural joint, Cedar City.	49
42.	Shear stress-normal stress for natural joints (Cedar City) sheared under either one or several direct shear load cycles.	50
43.	Cumulative shear stress-normal stress for natural, saw-cut and Brazilian joints (Cedar City) sheared under various load paths.	50
44.	Shear stress-normal stress for natural, saw-cut and Brazilian joints (Cedar City) sheared under 30° load path.	51
45.	Shear stress-normal stress for natural, saw-cut and Brazilian joints (Cedar City) sheared under 45° load path.	51
46.	Schematic of surface roughness and contact area effects versus friction angle.	52
47.	Natural joint (Cedar City) with low contact area.	52
48.	Saw-cut joints (Cedar City) sheared under various load paths.	54
49.	Natural joints (Cedar City) sheared under various load paths.	54
50.	Typical <i>in situ</i> stress-strain data for Cedar City quartz diorite.	56

51.	Shear stress versus displacement for joints with different surface areas. All specimens had a single joint oriented 45° to axis of loading.	58
52.	The decrease in strength as a function of specimen size for diorite and sandstone.	62
53.	Size effects for a variety of rock types.	62
54.	Maximum shear strength as a function of joint area. Specimens have a single joint.	66
55.	Stress-displacement diagram showing the contribution of individual joints and the average displacement (S_1) of the "intact" rock to the total shortening of the entire block. In terms of displacement: $D_2 = D_4 + D_5 + D_6 + S_1$.	66
56.	Comparative stress-strain curves showing the relative contributions of elastic, microfracture and joint deformation.	68
57.	Compression (a) and shear (b) behavior of joints as a function of stress (σ) and displacement ($\Delta\mu_0$). (Ref. 36).	69
58.	Variation of modulus ratio with RQD (a) velocity ratio (b). (Ref. 24).	70
59.	Failure envelopes for intact and jointed modeling material (after 10).	72
60.	Shear stiffness as a function of joint surface area. Dashed line represents range of other published data (Ref. 7).	74
61.	Shear stiffness as a function of normal stress.	75

LIST OF TABLES

<u>Table No.</u>	<u>Description</u>	<u>Page</u>
I.	Potential Test Sites.	4
II.	<i>In Situ</i> Test Series.	15
III.	Test Matrix - Mixed Company.	16
IV.	Summary of Laboratory Shear Tests.	40

SECTION I

INTRODUCTION

The objectives of the current program were: (1) to compare deformation and friction data derived from the Terra Tek test technique with data from other types of *in situ* tests, (2) to evaluate this technique in a variety of rock types, structural configurations and under conditions typical of field sites, (3) to conduct a series of field and laboratory tests to study the effects of specimen size, anisotropy and saturation on the strength and deformation of the rock and relate this and other data to the *in situ* and laboratory tests.

The determination of the *in situ* properties of a rock mass is a prerequisite for predicting its response to static or dynamic loads. The accuracy of calculations of stress and displacement is only as good as our measurement of rock mass properties. The rock mass will consist of intact blocks or layers separated by structural discontinuities such as joints, bedding planes or faults. Adequate modeling of the response in rocks with sharp structural discontinuities, therefore, requires determination of: (1) intact properties of the rock, (2) frictional properties of the discontinuities and (3) block interaction phenomena. The methods for obtaining the required rock and soil properties are field tests,^{1,2} laboratory tests³⁻⁶ and model studies⁷⁻¹⁰ simulating jointed rock masses.

In determining these properties, the concept of "scale or size effect" must be considered with respect to both "intact" and jointed specimens if properties are to be meaningful.² In addition, the "homogeneity" of the material with respect to strength, deformation and stress-wave propagation should be ascertained.

Mathematical models for "intact" rock, concrete and soil have been developed using elastic ideally-plastic,¹¹ variable moduli^{12,13} and cap models.¹⁴ Nonlinear constitutive equations have been developed by Herrmann and Nunziato.¹⁵ Each of these models has various advantages and disadvantages toward fitting observed experimental phenomena such as yield compaction, work hardening, dilation and hysteresis; and being rigorous from a theoretical standpoint.⁵ Mathematical models that simulate rock mass response and account for discontinuities fall into two categories: (1) continuum models that include "degraded" properties to account for discontinuities^{16,17} and (2) discrete models,¹⁸⁻²¹ for either finite element or finite difference calculations, which try to account for the strength and moduli of the rock mass by incorporating properties of joints and other discontinuities as well as "intact" properties.

SECTION II

TEST SITE LOCATIONS

Several sites at which the United States Bureau of Reclamation had conducted *in situ* direct shear, radial jacking or other *in situ* dynamic tests were investigated as potential test sites (Table I). These dam sites included Grand Coulee, Washington; Dworshak, Idaho; Yellowtail, Montana; Auburn, California; Morrow Point and Twin Forks, Colorado; Flaming Gorge, Utah and Glen Canyon, Arizona. Three sites were selected--Auburn, Morrow Point and Glen Canyon--based on: (1) available field test data, (2) rock type and geologic structure, (3) availability of test site locations and (4) logistical considerations.

Morrow Point Damsite

The Morrow Point complex located 20 miles east of Montrose, Colorado, on the Gunnison River, is comprised of a double-curvature, thin arch dam and associated underground powerplant.¹⁵ The power plant chamber was excavated in the wall of the left abutment, 400 feet below the ground surface. The rock at the damsite consists of irregular lenticular beds of Precambrian quartz-mica shist, mica shist and micaceous quartzite which has been intruded by granitic pegmatite. The rock mass is both heterogeneous and anisotropic due to the variability in rock type, highly developed foliation and pervasive joint sets (Figure 1). *In situ* tests were conducted by the U.S. Bureau of Reclamation in exploratory adits in the left and right dam abutments. Direct shear and sliding friction tests and uniaxial jacking tests were conducted to obtain frictional and deformational properties, respectively.

Table I. Potential Test Sites

<u>Site</u>	<u>Location</u>	<u>Structure</u>	<u>In-situ Test Conducted</u>	<u>Rock Type</u>	<u>Comments</u>
Auburn	California	double curvature arch structure (not built)	direct shear, radial and uniaxial jacking, plate jacking and stress relief	Amphibolite	Conducted tests in exploratory tunnels.
Grand Coulee	Washington	power plant	direct shear	Granite	Area previously tested now excavated. No other suitable area available.
Dworschak	Idaho	dam (double arch)	deformation test	Gneiss	Dam near completion. No outcrops or tunnels available.
Yellowtail	Montana	dam (single arch)	deformation tests	Limestone	Adits where tests previously conducted now grouted.
Morrow Point	Colorado	power plant and double curvature arch dam	direct shear seismic velocities uniaxial jacking	Precambrian Mica Schist and Quartzite	Only 30° dip slope available near left abutment; was too broken up because of blasting to conduct tests.
Glen Canyon	Arizona	single arch dam, access tunnel and portals	uniaxial jacking	Navajo Sandstone	Conducted tests in adits off of service road.
Mixed Company	Colorado	high explosive test series	dynamic test, velocity, acceleration	Kayenta Sandstone	Tests on surface outcrops of sandstone.
Two Forks	Colorado	exploratory adits	uniaxial jacking radial jacking	Precambrian Greiss and Amphibolite	Only one exploratory tunnel, no logistics.



Figure 1. Highly foliated Precambrian schist and gneiss, Morrow Point Dam, Colorado.

In addition, seismic velocity measurements were used to calculate the *in situ* modulus over large volumes of rock.

An attempt was made by Terra Tek to conduct an *in situ* shear test on a jointed specimen located on the sloping 30° surface at the left dam abutment. The rock was composed of interbedded quartz mica shist and micaceous quartzite. We were unable to excavate specimens for *in situ* tests because of the highly fractured nature of the material due to blasting. The area where the original U.S. Bureau of Reclamation (USBR) tests were conducted had been either destroyed or subsequently grouted during the construction phase of the project. In addition, cores were also taken to provide specimens for laboratory tests.

We decided to abandon the Morrow Point site and to conduct a test series at the Mixed Company test site.

Mixed Company Test Site

The test site for the Mixed Company program, a series of high-explosive experiments, is located 17 miles west, southwest of Grand Junction, Colorado. The site is situated on the broad plane of the Uncompahgre Plateau; part of the Colorado Plateau physiographic province. The stratigraphic column at the site is composed of a flat lying sedimentary sequence of sandstones, siltstone and conglomerates (Figure 2). The Precambrian basement is found at a depth of 500 (± 50) feet. The Kayenta formation, which outcrops at the surface of the site, consists of massive to thin beds of sandstone, siltstone and conglomerate with occasional layers of shale.¹⁶ The unit is approximately 70 feet thick. Our test site was located in a flat exposure approximately 300 feet from the Air Force Weapons Laboratory CIST experiment

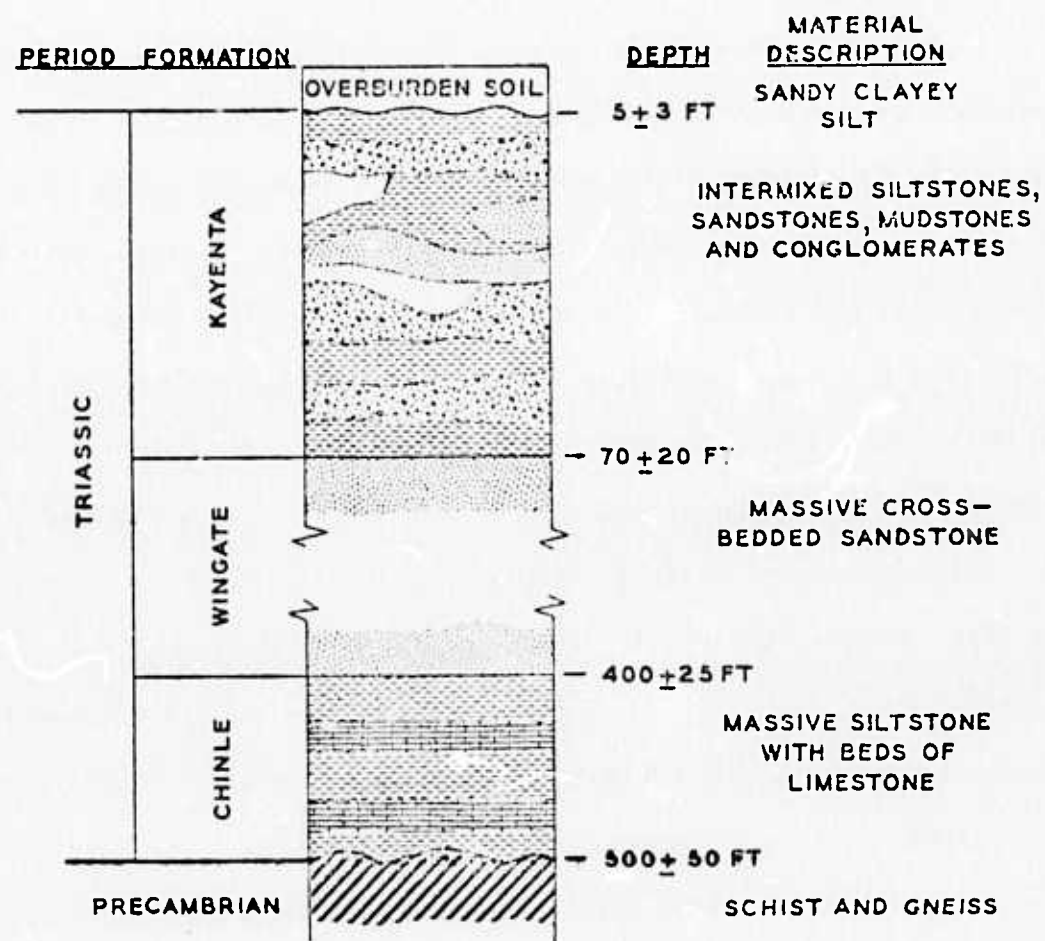


Figure 2. Stratigraphic section at the Mixed Company test site.

(Figure 3). The medium-grained sandstone member tested by Terra Tek was 6 to 8 feet thick and was relatively homogeneous over the test area of interest (Figure 4).

Auburn Damsite

Auburn dam, located on the North Fork of American River, 40 miles northeast of Sacramento, California, will be a double-curvature arch dam. The foundation of the damsite consists primarily of foliated amphibolite with minor amounts of talc and chlorite schists. Faults, shear zones and several joint sets were found in both abutments. Extensive field and laboratory tests were conducted by the U.S. Bureau of Reclamation (USBR) to determine deformational and frictional properties of the foundation rock.¹⁷ *In situ* tests included direct shear and sliding friction tests on joints (Figure 5), radial and uniaxial jacking tests to obtain deformation modulus and overcoring techniques to measure *in situ* stress conditions. These tests were conducted in six exploratory adits. Laboratory tests, including triaxial and direct shear tests, were also conducted. In order to compare our testing technique with that of the USBR, a series of *in situ* and laboratory tests was conducted. The *in situ* tests consisted of uniaxial stress and direct shear tests on amphibolite and chloritic schist. The *in situ* tests were conducted in the exploratory tunnels in close proximity to the test areas used by the USBR (Figure 6). Cores of intact rocks and jointed specimens were also taken for the laboratory program which consisted of direct shear and sliding friction tests.

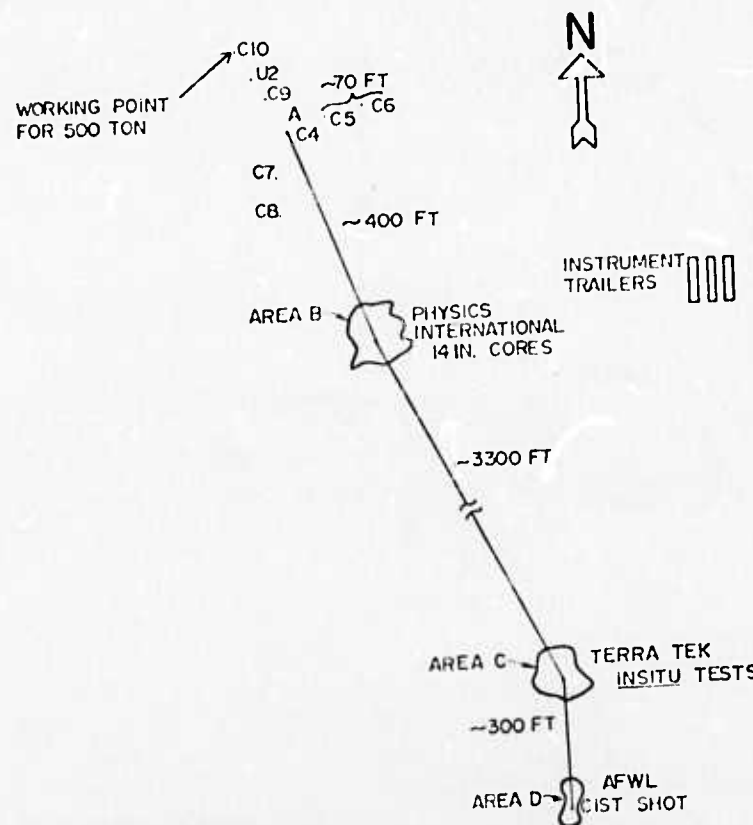


Figure 3. Test site location at the Mixed Company test site.



Figure 4. Drill rig is positioned for slotting of *in situ* specimen at Mixed Company test site. CIST site and cores in background.

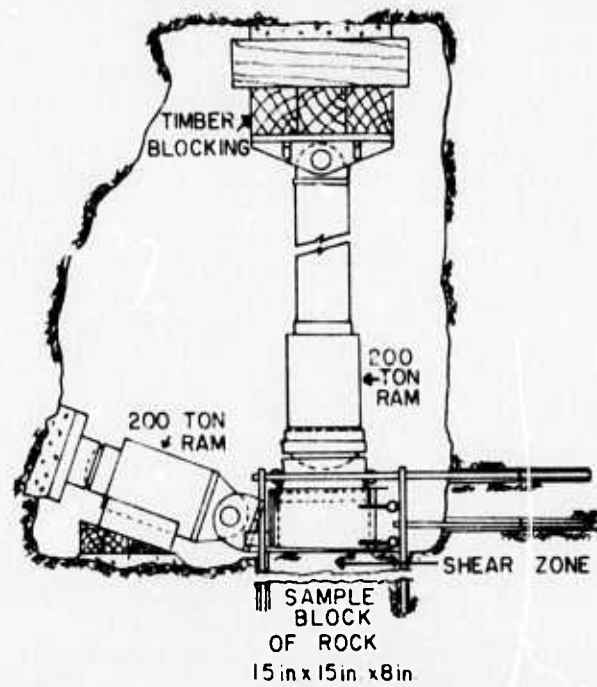


Figure 5. Schematic of U.S. Bureau of Reclamation *in situ* direct shear test, Auburn damsite, California. (Ref. 1)

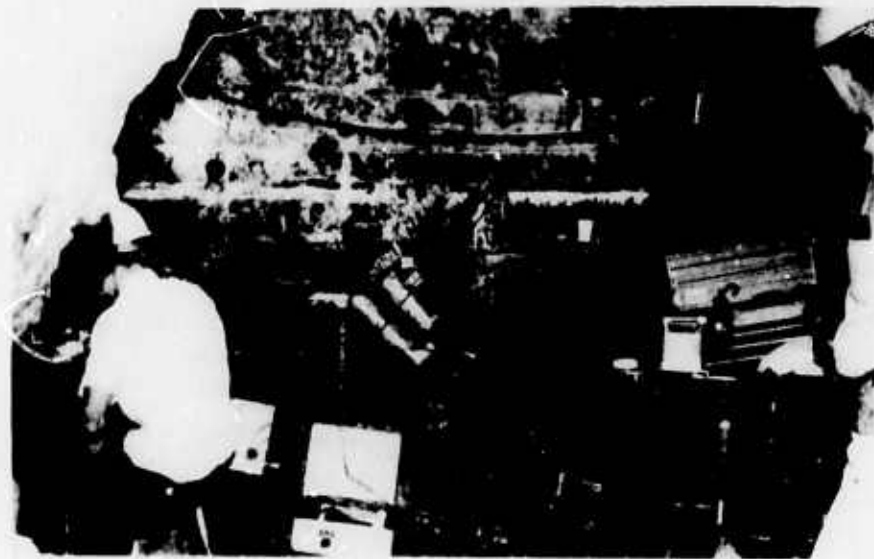


Figure 6. Instrumented *in situ* test in exploratory adit at Auburn damsite. Radial jacking test location (USBR) is seen at far right.

Glen Canyon Dam

The Glen Canyon dam and powerplant is located on the Colorado River, 2 miles from Page, Arizona. The foundation of the dam is situated in the Navajo formation; a coarse-grained cross-bedded sandstone (Figure 7). Bedding in the unit is very massive and the joint spacing is wide. The USBR has conducted a series of *in situ* shear and uniaxial jacking tests to determine friction and deformation of the rock. In addition, they conducted laboratory triaxial and direct shear tests. A series of *in situ* and laboratory shear tests was conducted on both the joints and cross beds in adits associated with the service road leading from the dam to the top of the canyon (Figure 8) and located near sites where the Bureau conducted shear tests.



Figure 7. Massive cross-bedded Navajo sandstone located at Glen Canyon, Arizona.



Figure 8. Test site location in adit at Glen Canyon dam.

SECTION III

TEST PROGRAM

Field Program

The *in situ* test program was conducted at the four field sites previously discussed: (1) Auburn damsite, California; (2) Mixed Company test site, Colorado; (3) Morrow Point damsite, Colorado and (4) Glen Canyon damsite, Arizona. The studies at the sites consisted of *in situ* shear and deformation tests on samples ranging from 12 to 66 inches in length. The tests are summarized in Table II. The tests were conducted under a wide variety of field conditions including the excavation of large samples on slopes up to 30° (Figure 9) and smaller samples on vertical walls in exploratory adits (Figure 10). Rock types at the sites (which included amphibolites, gneisses, shists and sandstones) varied greatly in their response to loading. The structural environment also varied significantly, ranging from massive sandstones to highly contorted and fractured gneiss and amphibolite.

Laboratory Program

Laboratory studies were also conducted at the various sites. Direct shear tests were conducted on 6-inch cores containing natural undisturbed joints from Auburn, California, Cedar City, Utah, and Page, Arizona. Specimens of Navajo sandstone from Page, Arizona, containing natural crossbeds were tested to determine whether the crossbeds could or do act as planes of weakness in the massive unit.

In addition to the field tests at the Mixed Company site, a series of uniaxial and triaxial compression tests were conducted on "intact"



Figure 9. Test location and drilling rig at Morrow Point dam, Colorado.

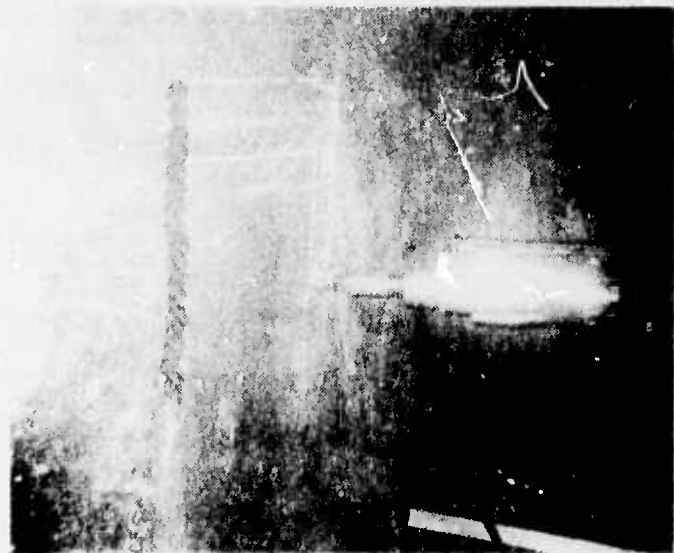


Figure 10. Specimen of chloritic schist being excavated on vertical wall, Auburn dam, California.

specimens of Kayenta sandstone ranging in diameter from 3/4 to 6 inches (Table III). The objectives of this study were to study the effects of specimen size, degree of saturation and variation in porosity on strength and deformation. Approximately 65 tests were conducted on this part of the program.

A series of servocontrolled direct shear tests along various load paths was conducted on natural and prepared surfaces of Cedar City quartz diorite. The objectives of the direct shear tests on Cedar City quartz diorite were: (1) to simulate the load paths followed in the field tests conducted on large specimens and (2) to determine the effect of load path on both the ultimate shear strength and shear stiffness on natural and prepared surfaces of various roughnesses.

Table II. *In Situ* Test Series

<u>Test No.</u>	<u>Site</u>	<u>Test Location</u>	<u>Test Size (inches)</u>	<u>Angle of Joint to Load</u>	<u>Comments</u>
1 2	Auburn Damsite	Auburn, Calif. Auburn, Calif.	12 x 18 12 x 18	45° joint intact specimen	amphibolite chloritic schist
3	Mixed Company Test Site	Grand Junction, Col.	6 x 12	intact specimen	sandstone
4		Grand Junction, Col.	12 x 24	intact specimen	
5		Grand Junction, Col.	24 x 36	intact specimen	
6		Grand Junction, Col.	36 x 72	intact specimen	
7	Morrow Point Damsite	Morrow Point, Col.	18 x 36	45° joint	schist and quartzite
8	Glen Canyon Damsite	Page, Arizona	6 x 12	45° joint	sandstone
9		Page, Arizona	12 x 24	45° joint	
10		Page, Arizona	12 x 24	intact specimen	
11		Page, Arizona	18 x 36	intact specimen	

Table III. Test Matrix - Mixed Company

In Situ Tests

Size (in)	Failure Stress (psi)	Strain at Failure ($\mu\epsilon$)	$E_{tan 50} \times 10^6$ psi	Poisson's Ratio	Comments
12 x 24	1630 (1740)	1860	1.04	.32	(17.5% water content) damp; unevenly loaded
18 x 36	2190	1540	1.99	.37	good test
24 x 48	925	860	1.92	-	unevenly loaded
36 x 72	1730	1465	1.97	.13	good test

Laboratory Tests

Size (in)	Orientation	Saturation	Number Of Tests	P_c (kb)
3/4 x 1 1/2	Parallel Perpendicular	0	4	0
		0	15	0
		25	2	0
		50	2	0
		75	2	0
		100	3	0
3/4 x 1 1/2*	Perpendicular	0	9	.5
		0	5	2
		0	11	4
2 x 4	Parallel Perpendicular	0	4	0
		0	5	0
6 x 12	Perpendicular	0	3	0

* Tests conducted for a DNA program.

SECTION IV

EXPERIMENTAL TECHNIQUES

Specimen Preparation

The *in situ* specimens were prepared by the drilling techniques and equipment previously developed. Briefly, three slots, two at 60° to the surface of the outcrop to form the sides of the specimen and one vertical slot to form the end of the specimen, are cut by a drilling technique (Figure 11). In this technique a row of 1 1/2-inch diameter holes are drilled on 2 1/2-inch centers; the web between the holes is subsequently removed by a drill situated between guides. Jointed specimens are prepared by first cutting a single 60° slot, backfilling with sand, then cutting the 6-inch wide vertical end slot. After the flatjack package is grouted in place the hydrostone allowed to harden, the final slot is cut in a manner similar to the first. Specimens 12 x 24 inches and smaller were prepared using a template bolted to the surface of the rock. The template accommodates a 3/4-inch carbide drill with holes spaced 1/2 inch apart. The webs between the holes are subsequently broached using a power impact chisel.

At the Auburn damsite the *in situ* specimens had to be diamond cored because of the composition and structural complexity of the rock. In addition, a special reaction frame had to be designed to excavate the samples in the exploratory tunnels (Figure 12).

The surface of the specimen is prepared for strain gaging by grinding the surface smooth, filling holes and pits with epoxy and regrinding and sanding to attain a final, smooth surface.



Figure 11. Drilling rig and partially prepared *in situ* specimen. Flatjack package at left.

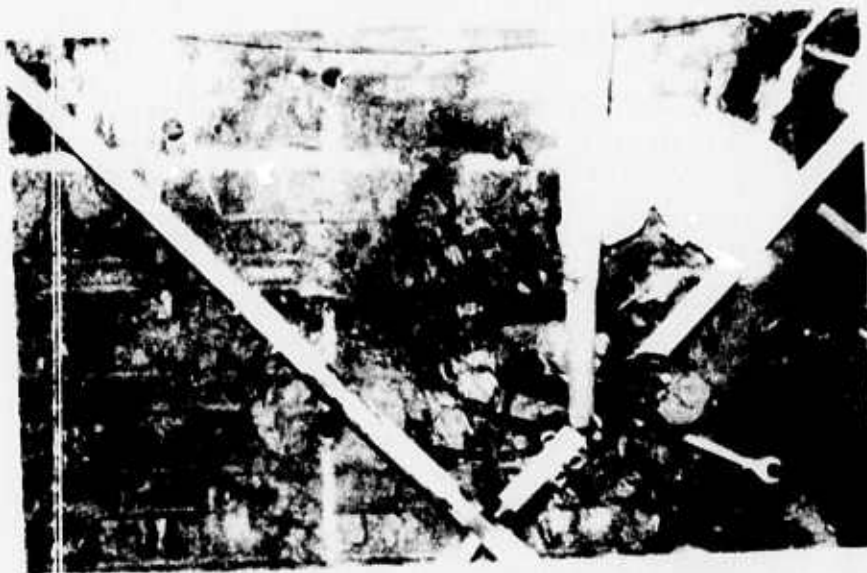


Figure 12. Special drilling frame developed for specimen preparation in the Auburn damsite exploratory adit.

The laboratory specimens were cored from the same joints as were tested *in situ*. Prior to breaking the core from the host rock, the specimens were banded so that no movement would occur along the joint. Each 6-inch diameter core was at least 6 inches long. During all cutting procedures in the laboratory, the joint was sealed so that water could not penetrate the joint, thus changing its character. Solid NX core was taken at several locations. These cores were either cut in half lengthwise by a diamond saw providing a direct shear specimen with a surface relief of about 600 to 700 microinches, or broken in a Brazilian tension test to provide a fresh surface with a relief of about 0.1 to 0.2 inch. The specimens were then cast in hydrostone prior to testing in direct shear. Intact specimens were cored using conventional procedures.

Loading System

The system used to apply the axial load to the *in situ* system consisted of a flatjack package pressurized by a hydraulic system. The package consisted of three triangular stainless steel flatjacks sandwiched between two triangular 2-inch steel plates. Details of the flatjack construction and method of calibration of efficiency as a function of pressure and size is described in Reference 2. A pneumatic-hydraulic pumping system was fabricated to supply water containing water-soluble oil to the flatjacks in the loading package (Figure 13). Pressure was supplied by 1100 psi and 6600 psi Sprague pumps and monitored by 10,000 psi Crosby Bourdon tube gages and 1000, 5000 and 10,000 psi pressure transducers.

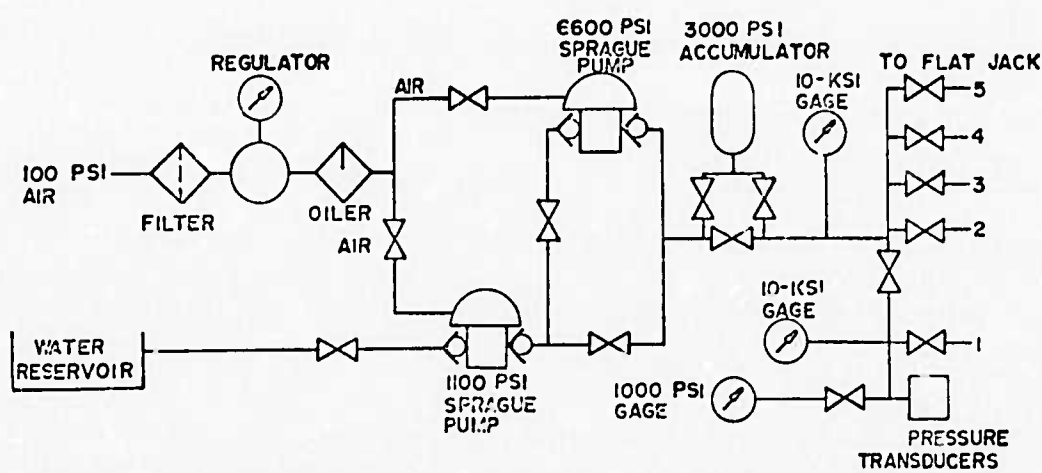


Figure 13. Schematic of the pneumatic-hydraulic pumping system.

Instrumentation

In Situ Tests

The pressure applied to the joint specimen was measured by 10,000, 5000 and 1000 psi transducers. Direct Current Differential Transducers (DCDTs) measured total axial strain and shear displacement along the joint. Output from the pressure transducers, DCDTs and linear potentiometers was monitored on a 9-channel oscillograph recorder and X-Y recorder. Micromeasurement 20 CBW, 2-inch gage length, foil strain gages were placed axially and transversely at several locations on the top of the specimen. All gages are water proofed and temperature compensated.

Strain gage output was channeled through a 12-channel bridge balance to a 24-channel recorder. A schematic of the instrumentation is shown in Figure 14.

Laboratory Tests

The direct shear tests were conducted on a 235-kip, servo-controlled direct shear machine (Figure 15). Normal and shear stresses are applied by independently controlled 235-kip cylinders. This closed-loop system makes it possible to keep the normal stress constant or vary it at will throughout the test. Maximum shear displacement allowed is 3 inches, but in most tests, maximum displacement was 0.1 to 1 inch. Unique features of the test equipment include an oil bearing instead of roller bearings to reduce friction and an alignment scheme to prevent rotation during the test. Normal and shear stresses are monitored by calibrated load cells; shear displacement by a single DCDT and the vertical displacement by two DCDTs, one mounted on either side of

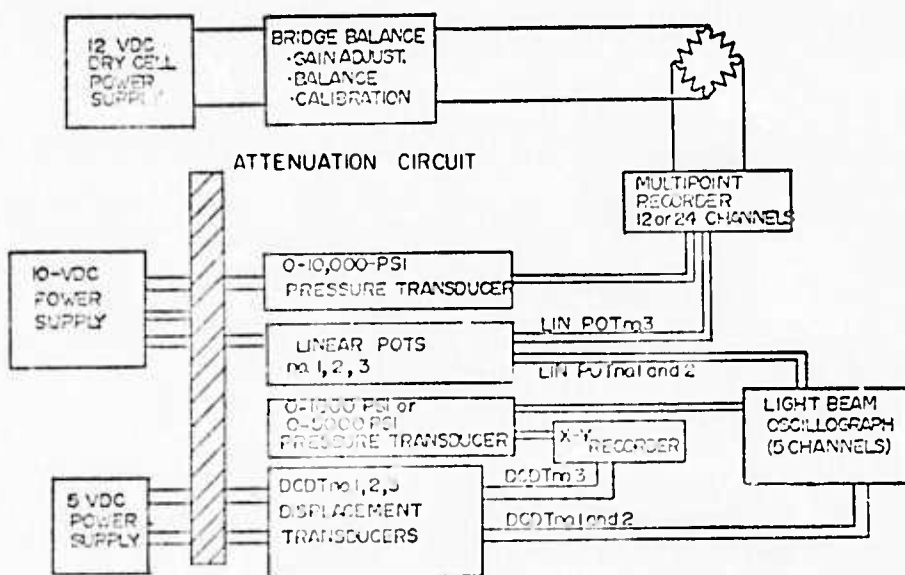


Figure 14. Schematic of instrumentation layout.

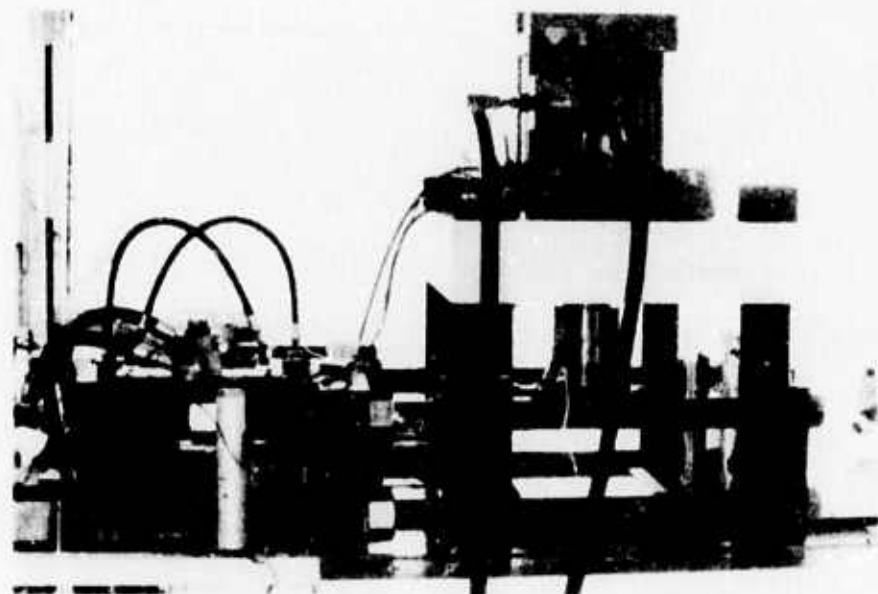


Figure 15. Servo-controlled direct shear machine.

the shear box. Normal stress, shear stress and shear displacement are plotted on an X-Y-Y' recorder.

All data is inputed into a Digital PDP 11 computer. From shear stress and normal stress displacement data, shear and normal stiffnesses are computed. An example of the computer output from a typical test is shown in Figure 16.

TEST # 1704

SIGMA1	SIGMA1-2	SHEAR DISPL	NOR DISP1	NOR DISP2
- .9068327	.2957042E-7	.2071455E-3	.2181509E-3	.517654E-4
198. 1836	.2477812	.8538997E-2	.3618432E-1	.4044172E-2
401. 0967	.4334827	.973107E-2	.4934104E-1	.0169014
526. 9894	.4333981	.1055442E-1	.5614753E-1	.2353384E-1
625. 17	.2483101	0	0	0
626. 2598	2. 91701	.828582E-3	.1114293E-2	.4535943E-2
623. 0695	.87. 53526	.276194E-3	.1181419E-2	.4612591E-2
625. 120	.150. 2347	.1841291E-2	.1476774E-2	.5001631E-2
623. 1558	.222. 5224	.4004812E-2	.1919006E-2	.5492603E-2
622. 3302	.272. 3164	.0064223	.2322563E-2	.3959491E-2
626. 0154	.314. 8483	.8562014E-2	.2926698E-2	.6464264E-2
623. 7168	.338. 4091	.1077157E-1	.3356205E-2	.6710089E-2
625. 0478	.351. 6759	.1292509E-1	.3624809E-2	.6952444E-2
624. 9195	.370. 7779	.1528273E-1	.3933589E-2	.7046565E-2
626. 2816	.387. 5822	.1763038E-1	.4215519E-2	.7168919E-2
628. 2964	.408. 6072	.2200345E-1	.4739103E-2	.7536236E-2
623. 1858	.424. 8092	.2642256E-1	.519556E-2	.7797162E-2
623. 1717	.444. 8756	.0337417	.5571466E-2	.7952459E-2
624. 6198	.457. 2186	.3871319E-1	.6041749E-2	.8224227E-2
624. 8033	.469. 6417	.4409297E-1	.6390763E-2	.0102172
625. 8439	.474. 5727	.4962265E-1	.6712968E-2	.0104272
625. 4644	.481. 2224	.5777058E-1	.9196276E-2	.1068208E-1
626. 6121	.487. 2759	.6392891E-1	.9545331E-2	.1090308E-1
623. 9690	.491. 0107	.7263902E-1	.9840606E-2	.1096772E-1
624. 83	.494. 2853	.882582	.1021609E-1	.1108427E-1
622. 5659	.497. 8132	.9226689E-1	.6105768	.1114897E-1
623. 6192	9. 641722	.8543601E-1	.1824487E-1	.1865400E-1
SIGMA1	SIGMA1-2	FRICITION <	NOR STIFF	SHEAR STIFF
- .9068327	.2957042E-7	.3260347E-7	-6719. 14	.2191009E-3
198. 1836	.2477812	.1250261E-2	9852. 698	.12. 31869
401. 0967	.4334827	.10801744E-2	12109. 96	.13. 08776
526. 9894	.4333981	.8224038E-3	13227. 4	.10. 87627
625. 17	.2483101	.3971881E-3	1	1
626. 2598	2. 91704	.4702932E-2	.219551. 8	.1032. 537
623. 0695	.87. 53526	.1404905	.215036. 6	.30210. 6
625. 120	.150. 2347	.2403263	.192982. 3	.46378. 71
623. 1558	.222. 5224	.3570886	.166115. 8	.60032. 41
622. 3302	.272. 3164	.4375754	.150284	.65760. 58
626. 0154	.314. 8483	.5029402	.133723. 8	.67053. 9
623. 7168	.338. 4091	.5426968	.123920. 6	.67251. 31
625. 0478	.351. 6759	.5629584	.119313. 2	.67169. 49
624. 9195	.370. 7779	.5933211	.113827. 1	.67536. 01
626. 2816	.387. 5822	.6198625	.109621. 2	.67970. 41
628. 2964	.408. 6072	.6503414	.102349. 8	.66562. 26
623. 1858	.424. 8092	.6816734	.95928. 43	.65391. 86
623. 1717	.444. 8756	.7138893	.92158. 41	.65790. 9
624. 6198	.457. 2106	.731995	.87570. 22	.64109. 96
624. 8033	.469. 6417	.7516633	.67154. 42	.50477. 51
625. 8439	.474. 5727	.7582925	.65361. 73	.49563. 3
625. 4644	.481. 2224	.7693842	.62926. 01	.48414. 28
626. 6121	.487. 2759	.7776354	.61287. 1	.47659. 62
623. 9690	.491. 0107	.7869142	.59972. 64	.47193. 33
624. 83	.494. 2853	.7910083	.58671. 82	.46489. 9
622. 5659	.497. 8132	.7996153	.57411. 7	.45907. 27
623. 6192	9. 641722	.1545595E-1	.33811. 5	.522. 589

Figure 16. Computer output from typical direct shear test.

SECTION V

TEST PROCEDURE

In situ Deformation Tests on Intact and Jointed Rock

The first flatjack next to the specimen is pressurized to approximately 0.25-inch displacement (total width of three jacks is 0.5 inch), which corresponds to a pressure of approximately 200 psi. The valving is arranged so that the front flatjack can be shut off from the rest of the system except for a direct line to the pressure transducer. This first jack is then used as a pressure cell for the rest of the test. Since it contains a fixed volume of fluid, its thickness does not vary significantly, thus eliminating this test variable. One purpose of the first jack is to "snug up" the flatjack package. The specimen is usually slightly strained at this time.

The second jack is then pressurized to a total width of 0.75 inch (0.58-inch displacement). If displacement along the joint or failure has not occurred before this displacement, the second jack is closed off and the third jack is pressurized to the same displacement. Displacement along the joint usually occurred during pressurization of this jack. Rate of loading was approximately 50 psi/minute. If failure of some type has not occurred at this point, then the valves to the second and third flatjacks are reopened and all the jacks except the front jack are pressurized simultaneously until failure of the rock or one of the flatjacks occurs.

Laboratory Tests

In the laboratory direct shear tests, the predetermined normal stress is applied by the vertical piston. For the "typical" direct

shear test, shear displacement rate is programmed and the shear stress, normal stress, shear displacements and vertical displacements are monitored. For "proportional-loading" direct shear tests, an initial predetermined normal stress is first applied. Then the shear stress and normal stress are applied so that the ratio of τ/σ_n is kept constant during loading until gross shearing occurred. For all tests, the normal stress was compensated as the contact area between blocks changed during displacement. A change in area of 1.6 percent occurs when a 6-inch x 6-inch sample is displaced 0.1 inch. Rate of shear displacement was approximately 0.10 inch/minute.

SECTION VI

EXPERIMENTAL RESULTS

Auburn Damsite

Both *in situ* and laboratory tests were conducted at the Auburn damsite (Table II). Deformation and frictional properties were measured on an amphibolite specimen containing a single joint and an "intact" chlorite schist specimen. The stress-strain response gives a modulus of 5.0 to 7.4×10^6 psi and $\nu = .29$ for the amphibolite (Figure 17). These modulus values are similar to those obtained by the USBR using a radial jacking test. They obtained moduli ranging from 5 to 10×10^6 psi at distances of 10 to 15 feet from the tunnel wall.¹

The frictional response of the amphibolite measured by us is comparable to that measured by the U.S. Bureau of Reclamation (USBR). The maximum shear strength (τ_m) at $\sigma_n = 700$ psi is 710 ± 20 psi for our test and 700 psi for a USBR test. Laboratory direct shear tests gave a friction angle (ϕ) of 38° for the rock tested by us; the USBR data gave a ϕ of 40° (Figure 18). The friction envelope developed from initial shear strength (τ_i) was non-linear at higher normal stress and fell significantly below maximum shear strength data. Shear stiffness calculated from the field and laboratory data (Figure 19) indicated that the field specimens were stiffer at comparable normal stresses. At $\sigma_n = 700$ psi, the field specimen had a shear stiffness of 34×10^3 psi/in while the laboratory specimen had a stiffness of 23×10^3 psi/in. Shear stiffness is defined as the slope of the shear stress-displacement curve. Each of these specimens contained only a single joint.

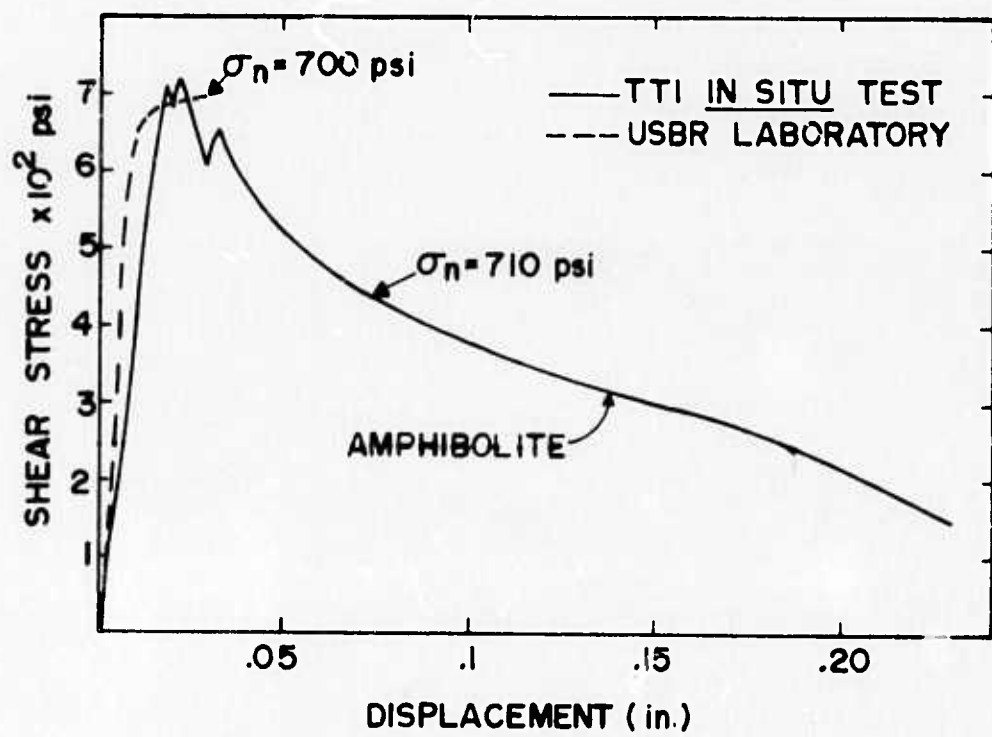
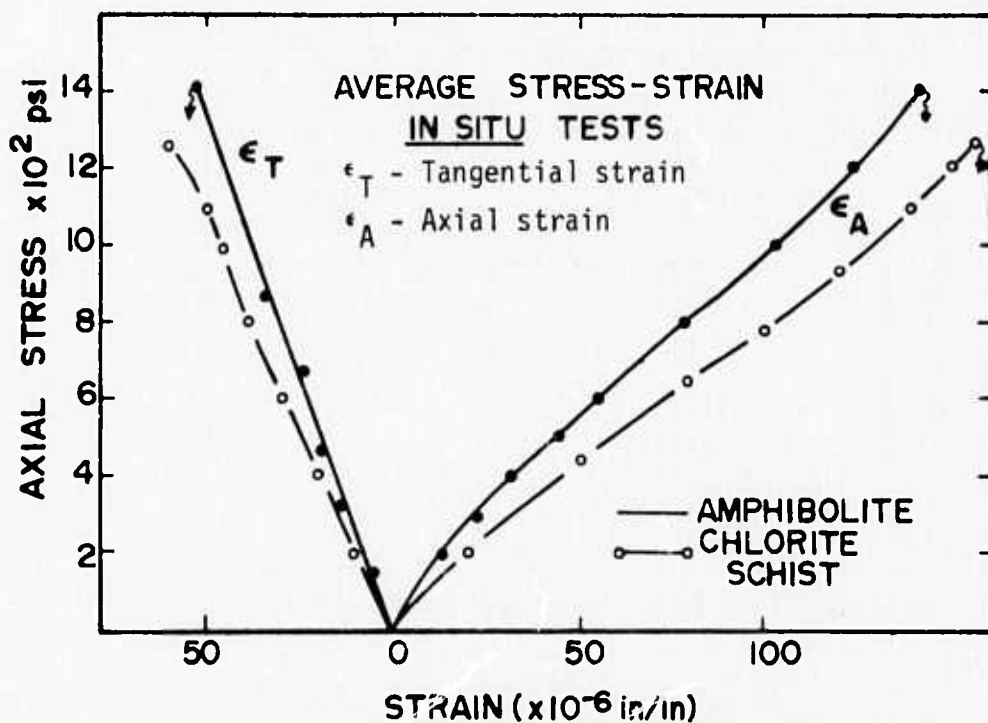


Figure 17. *In situ* stress-strain response of amphibolite and chloritic schist, Auburn damsite, California.

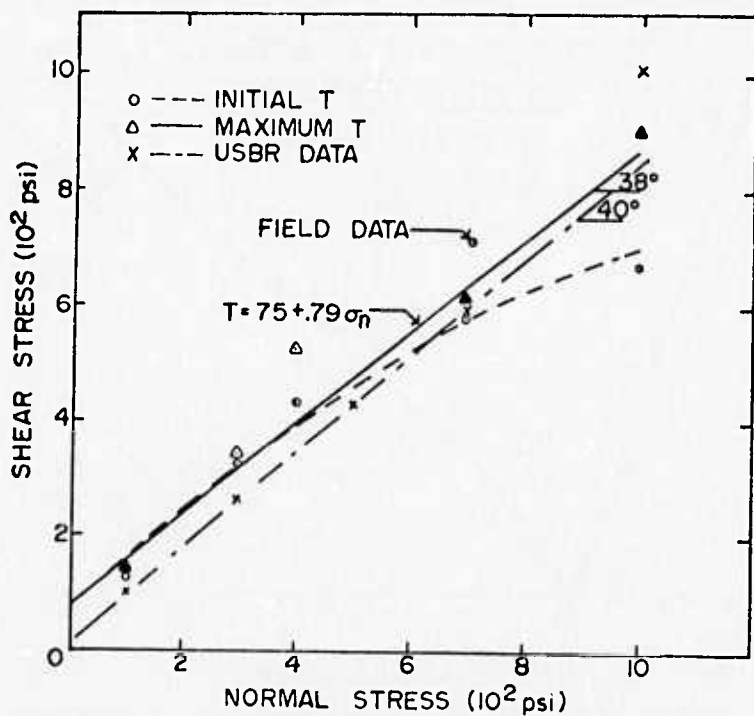


Figure 18. Friction envelopes for amphibolite, Auburn dams site, California.

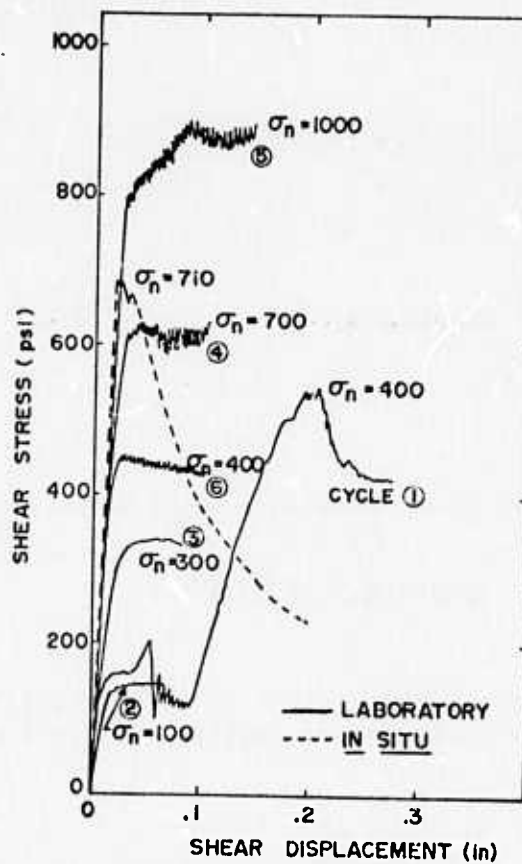


Figure 19. Shear stress versus displacement for field and laboratory tests, Auburn, California.

Mixed Company

An extensive series of *in situ* and laboratory tests were conducted at the Mixed Company test site (Table III). The field specimens ranged in size from 12 x 24 inches to 36 x 72 inches; the laboratory specimens from 3/4 x 1 1/2 inches to 6 x 12 inches. The objectives of the tests were to: (1) conduct a study to determine the effect of specimen size on strength and deformation, (2) study the effect of bedding orientation on strength and deformation, (3) study the effect of saturation on strength and deformation and (4) study effect of specimen density on strength. In reality, dry density is directly correlative with porosity since the sandstone is essentially monomineralic. The porosity of the specimens tested ranged from 15 to 27 percent.

Size Effects

Uniaxial stress tests were conducted over a range of effective diameters from .75 to 20 inches. The effective diameter is defined as the diameter of a right circular cylinder having the same volume as the triangular prism. Over this range the strength of the specimens decreased by a factor of 2 (Figure 20). However, the Young's modulus remained relatively constant, approximately 2.0×10^6 psi (Table III). All of these specimens were located parallel to the bedding.

Anisotropy

A series of unconfined compressive tests were conducted on specimens cored perpendicular and parallel to bedding to determine if the rock is anisotropic with respect to strength (Figure 21). The thickness of the bedding planes ranged from 0.5 to 2.0 inches. The strength of specimens

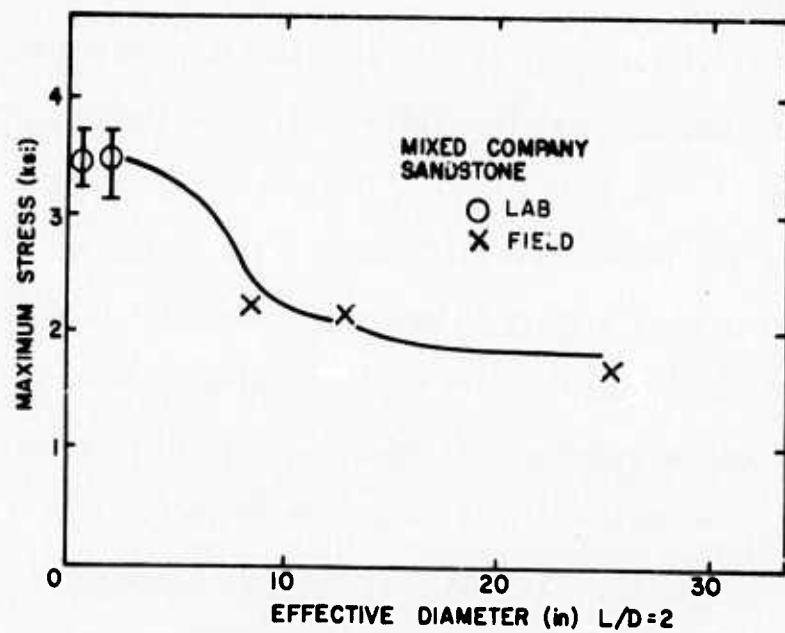


Figure 20. Effect of specimen size on strength for Kayenta sandstone, Mixed Company site, Colorado.

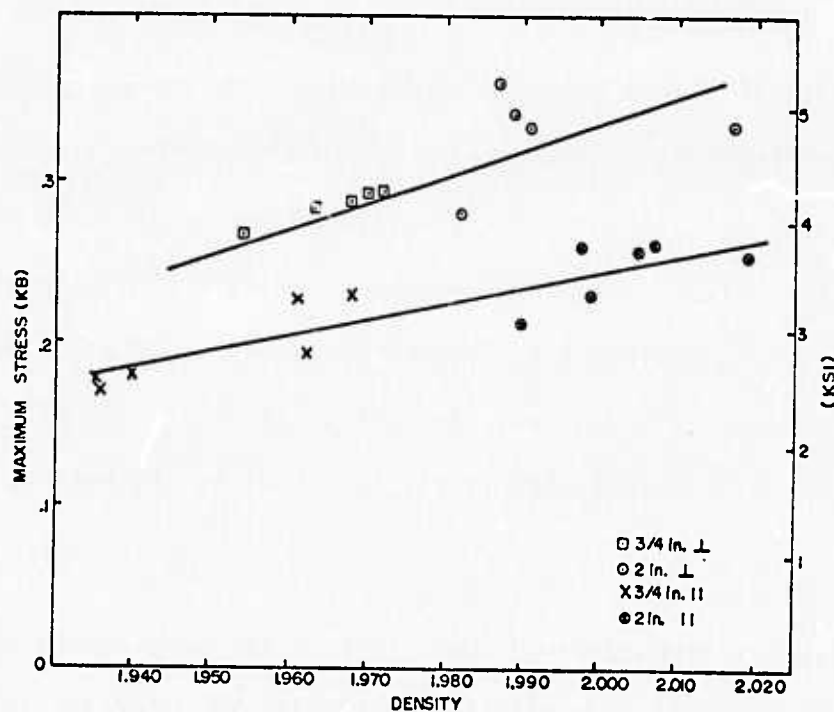


Figure 21. Strength as a function of density for specimen cored perpendicular and parallel to bedding.

tested perpendicular to bedding was significantly higher (25 percent) than those tested parallel to bedding. This trend in strength difference was found to be consistent over a range of densities noted for the Kayenta sandstone. On the other hand, the elastic modulus of the samples parallel to bedding was generally higher than the modulus of the samples perpendicular to bedding (Figure 22). Tests with bedding oriented 30° to the sample axis will be conducted in the future. Longitudinal velocity was measured on laboratory samples both perpendicular and parallel to bedding. The velocity measured perpendicular to bedding was 7080 fps compared to 8610 fps parallel to bedding; an anisotropy of 18%. This is in agreement with the modulus data mentioned above.

Effect of Saturation

The effect of saturation on unconfined strength and deformation was studied on small laboratory specimens. Saturation resulted in a reduction of strength from 4600 to 3300 psi (Figure 23a), approximately 28%. Because of the large data scatter at the higher percent saturation, it is difficult to determine whether there is decrease for specimens with greater than 75 percent saturation. The strain at failure appears to increase to a maximum at 60 percent of saturation, then decrease to a value approximately equal to the strain at failure for dry specimens (Figure 23b). The elastic modulus of dry specimens tends to be greater than saturated specimens, although data scatter is large (Figure 22).

Effect of Porosity

The effect of porosity on strength and deformation can be studied because density can be directly related to porosity since the Kayenta

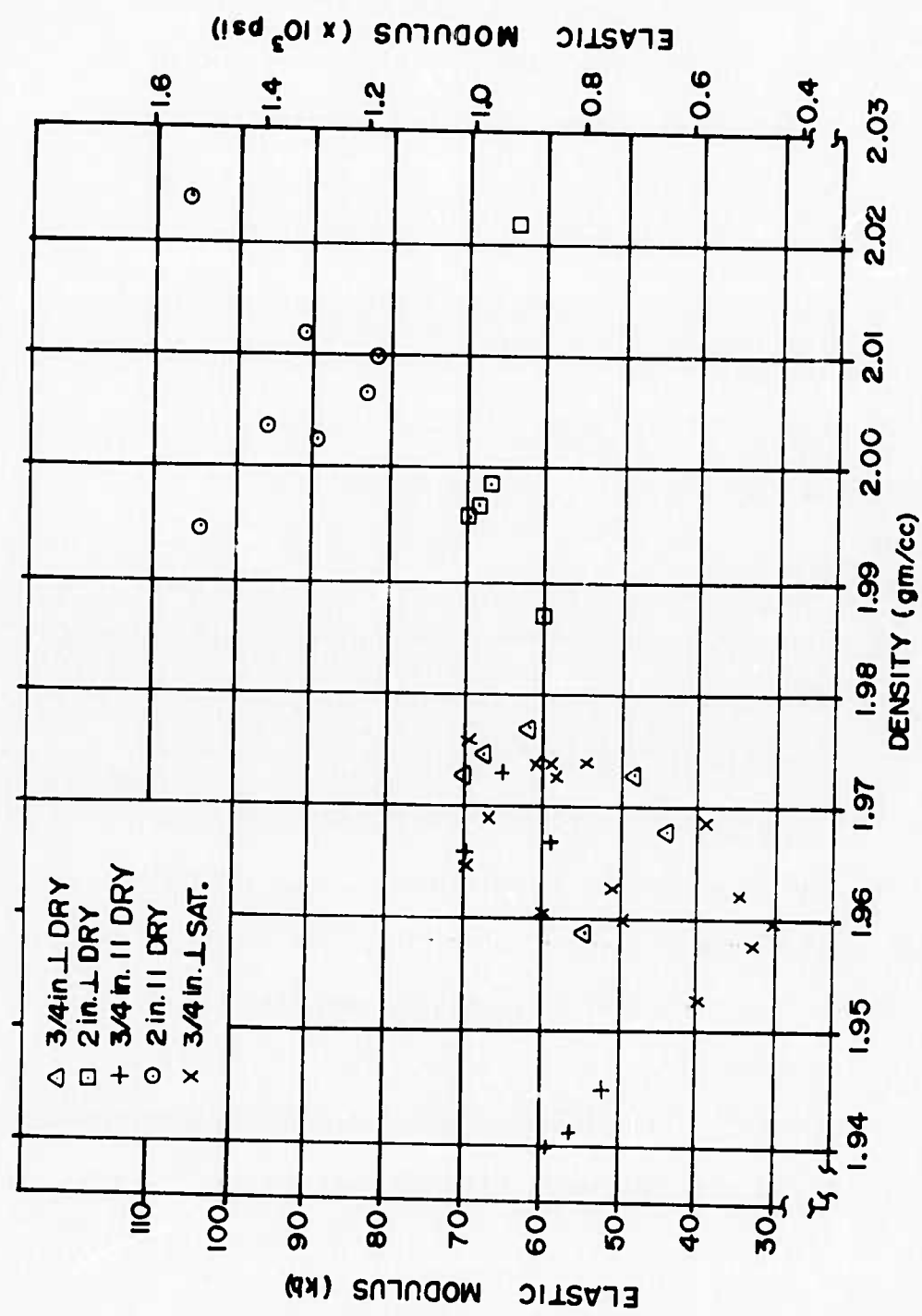
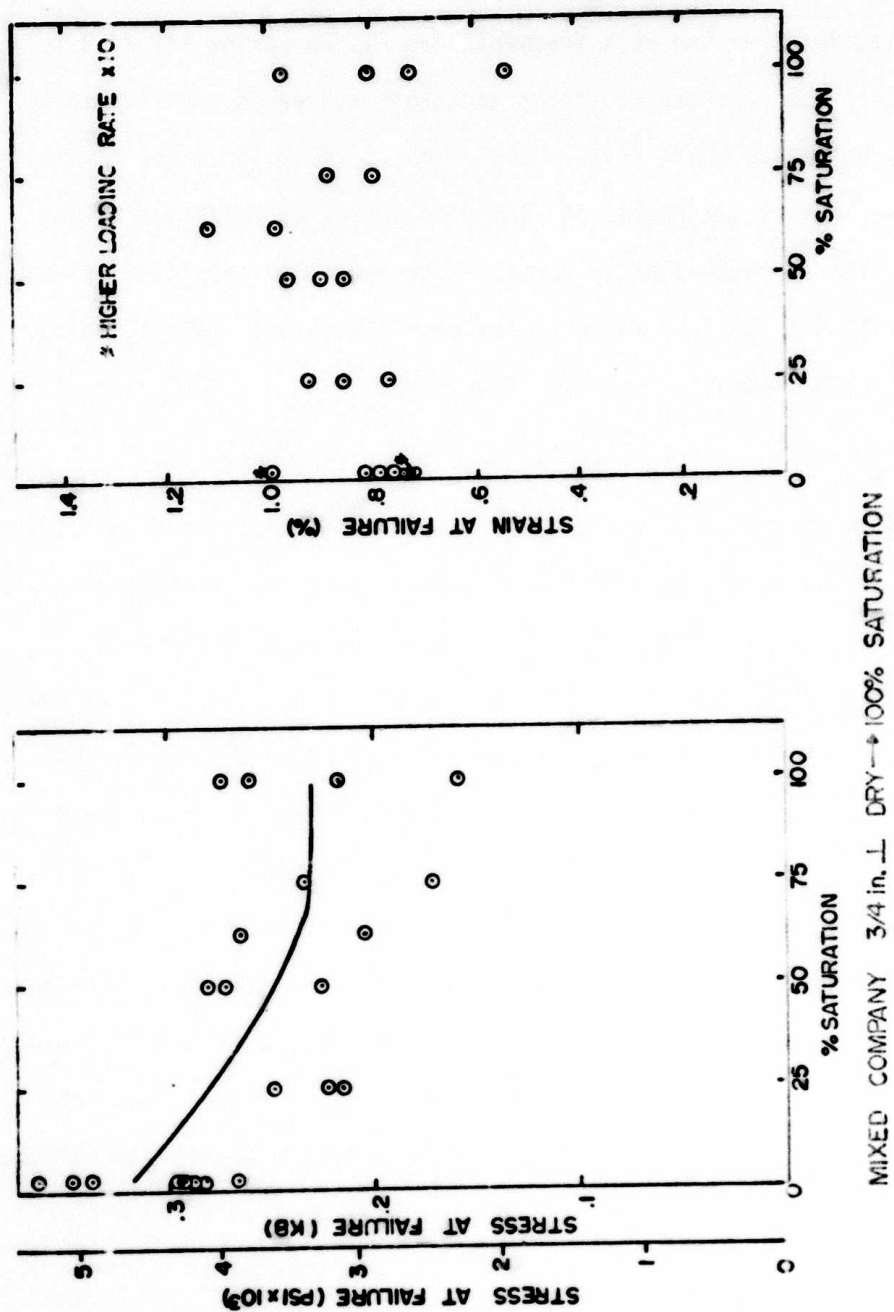


Figure 22. Elastic modulus as a function of density for specimens cored perpendicular and parallel to bedding.



sandstone tested is primarily composed of quartz with minor feldspar and rock fragments bonded with silica cement (Figure 24). The densities of the quartz, feldspar and rock fragments are all approximately 2.63 to 2.65 gm/cc. The strength of intact sandstone increased with confining pressures up to 4.0 kbars (Figure 25). The increase in strength with density was greater at higher confining pressures as indicated by the slopes in the strength-density curves. The range of porosities tested was calculated to be from 15 to 27 percent. The elastic modulus also increased with increasing density (Figure 25).

Glen Canyon

In situ tests were conducted on jointed and intact specimens located in adits of the access tunnel to Glen Canyon Dam. Two triangular prisms with natural joints oriented 45° to the specimen axis were sheared (Figure 26). The 8-inch by 12-inch specimen from adit #2 had very low joint contact prior to loading and consequently sheared to large displacement under relatively small shear stress. However, the maximum shear stress of the 8-inch by 12-inch specimen approached the residual shear stress of the 12-inch by 18-inch specimen. The 12-inch by 18-inch specimen sheared to a residual shear stress less than one-half its peak shear stress. Two intact specimens (Figure 27) were loaded to failure in uniaxial compression. The 18-inch by 34-inch specimen in adit #5 appeared to fail along bedding planes parallel to the prisms top surface while the 12-inch by 18-inch specimen in adit #2 sheared at an angle between 30° and 40° to the top surface. Failure occurred at a stress of 1500 psi. Adit #2 is located about 150 feet lower in the sandstone formation than adit #5 and contained denser and stronger rock.

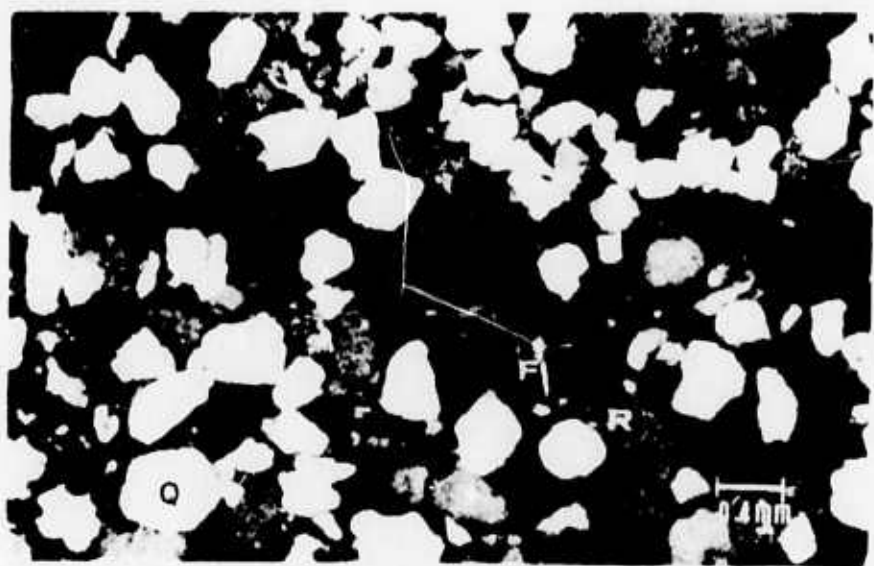


Figure 24. Photomicrograph of Kayenta sandstone (x 30)
 a. Plain light illustrating highly porous nature of material. b. Cross nicols.
 Dominant mineral present is quartz (Q) with minor feldspar (F) and rock fragments (R).

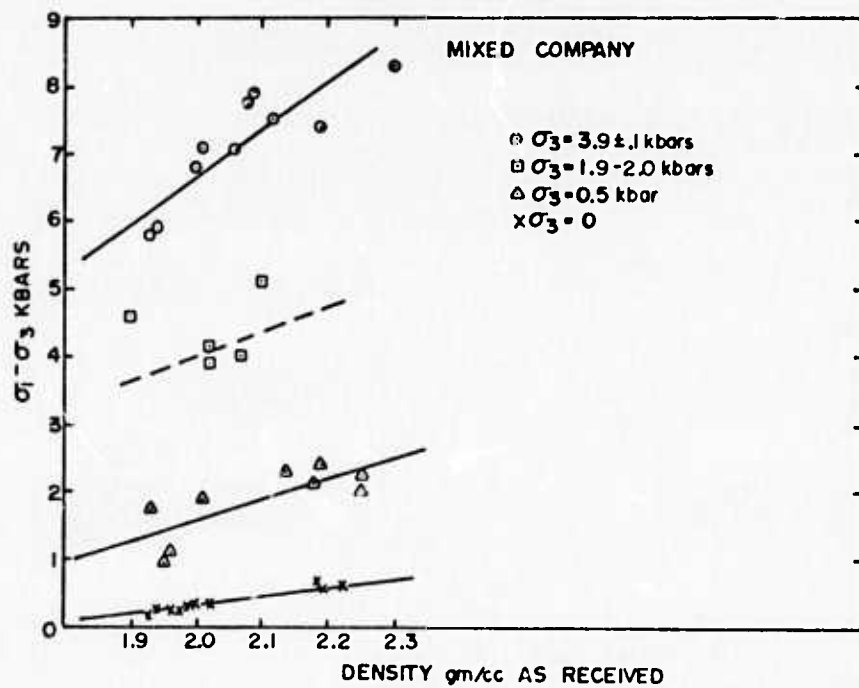


Figure 25. Stress difference as a function of density for triaxial tests up to $P_c = 4.0$ kbars.

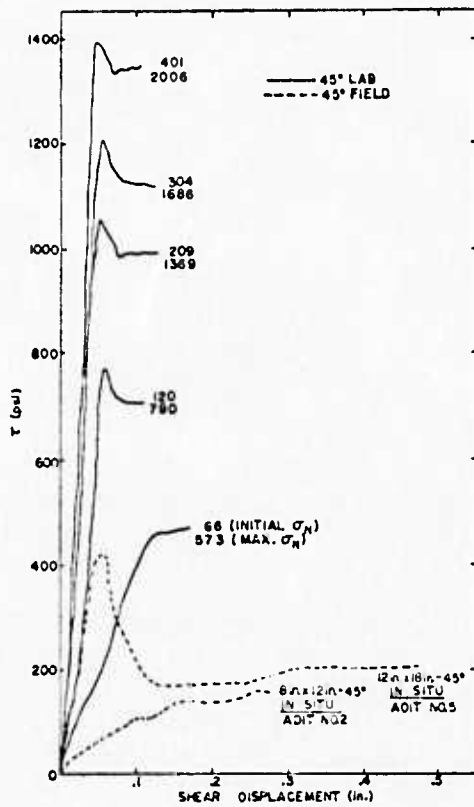


Figure 26. Shear stress-displacement for *in situ* and laboratory 45° proportional shear tests, Glen Canyon.

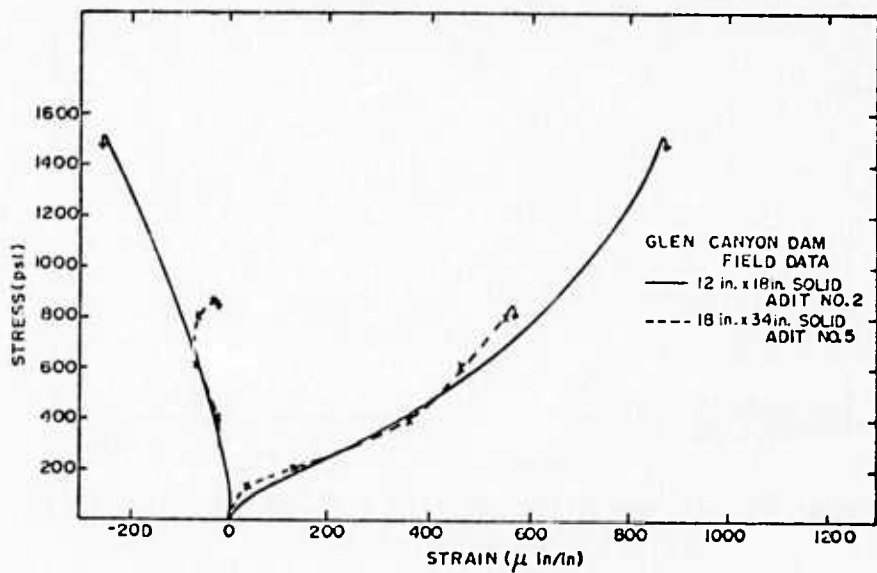


Figure 27. Stress-strain results for intact *in situ* specimen, Glen Canyon.

The *in situ* specimens had Young's moduli of 1.5 and 1.25×10^6 psi. These values are higher than the moduli obtained by uniaxial jacking tests conducted by the USBR in the left abutment. The moduli obtained by them averaged 1.0×10^6 psi for horizontally-oriented tests while vertically-oriented tests averaged 1.25×10^6 psi. Seismic tests conducted at the same location also average 1.25×10^6 psi.²² We conclude that our test results compare favorably with those of the U.S. Bureau of Reclamations. Results from the *in situ* shear tests conducted by the Bureau could not be located in the files of the USBR.

Natural joints were obtained for laboratory shear tests from the extension of the joints tested in the field. Both direct shear and proportional shear tests were conducted in the laboratory (Figure 28). In addition, cores were obtained from highly cross-bedded surface rock near the dam and sheared parallel to the bedding planes in the laboratory (Figure 29). The surprisingly large difference in the friction angle between the natural joint (42.1°) and the crossbed (32.6°) indicates that the crossbeds could very well act as planes of weakness if unfavorably oriented and if they individually extended over large areas. Uniaxial compression tests were also run on 3/4-inch diameter and 2-inch diameter cores oriented parallel and perpendicular to the bedding planes.

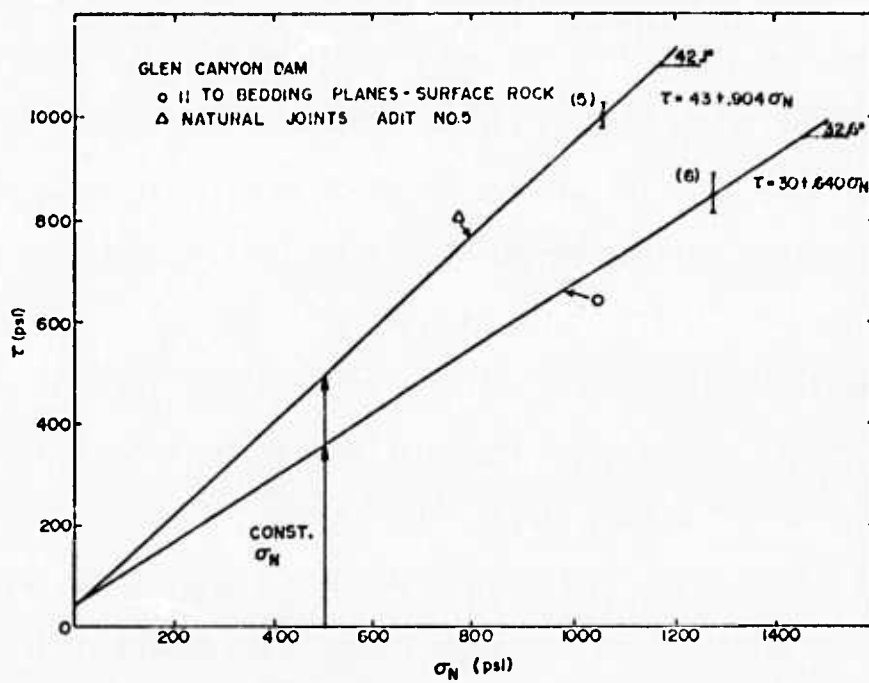


Figure 28. Relation of τ vs σ_N for *in situ* and laboratory direct shear and 45° proportional shear test, Glen Canyon.

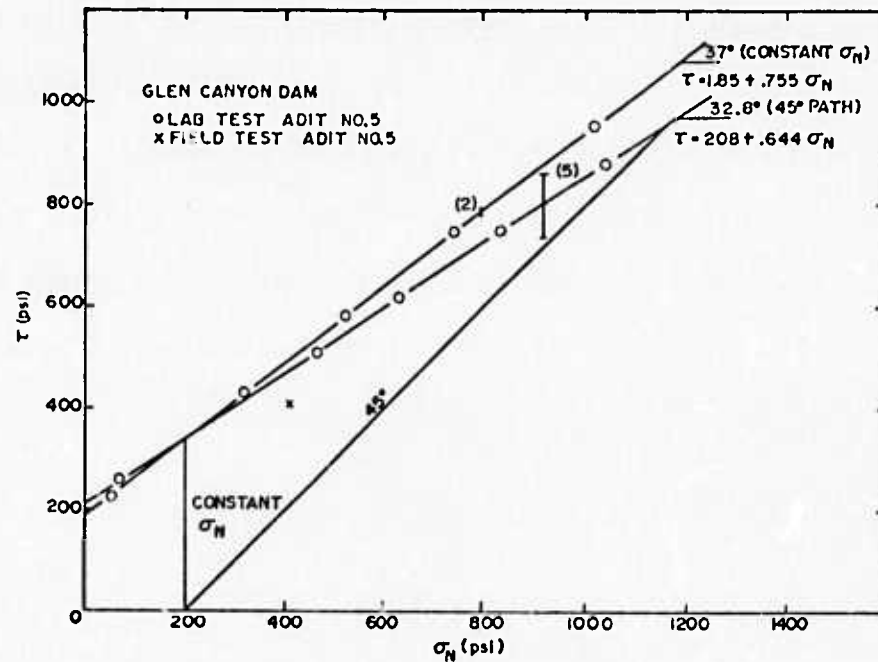


Figure 29. Comparison of τ vs σ_N for laboratory specimen with natural joints and bedding planes, Glen Canyon.

Cedar City Test Site

An extensive series of laboratory shear tests were conducted on natural joints and artificially prepared joints of Cedar City quartz diorite. Jointed specimens were sheared under a variety of loading paths and at several stress levels. Load paths included (1) direct shear loading where shear stress is applied after the specimen has been subjected to a predetermined normal stress, and (2) proportional shear loading where shear stress and normal stress are applied in a prescribed ratio after a low initial normal stress has been applied.

Twenty-two specimens were sheared under 164 loading cycles. Due to the limited number of specimens available, 11 previously sheared specimens were repositioned and sheared again. In addition, most virgin specimens were sheared at several initial normal stresses and, in some cases, under different load paths. In the latter case, a minimum amount of shear displacement was allowed after the maximum shear stress was reached. This reduced the effect of past loading on the next load cycle due to modification of the sheared surface. A summary of all laboratory shear tests is contained in Table IV.

Specimens containing natural joints were obtained by coring parallel to and centered over natural joints at the Cedar City, Utah test site. All specimens were cored from joints within a 20 x 20 foot area. Naturally jointed specimens sheared in the laboratory were approximately 5 3/4 inches in diameter by 6 inches long. Artificially jointed specimens were prepared from 2-inch diameter intact cores taken in the field near the jointed cores. The intact cores were either saw cut along the longitudinal

Table IV. Summary of Laboratory Shear Tests.

Load Path	Type of Specimen	Number of Specimens	VIRGIN			Number of Specimens	Standard Deviation psi	REPOSITIONED			Standard Deviation psi
			Number of Load Cycles	degrees	psi			Number of Load Paths	degrees	psi	
Constant on	Natural	5	12	.757	37.1	14	104	2	5	.535	28.1
	Natural [†]	18	18	.737	36.4	-2	79	8	11	.605	31.2
	Saw Cut	2	11	.711	35.4	30	32				22
45°	Natural	3	10	.654	33.2	88	35	3	24	.660	33.4
	Saw Cut	2	10	.663	33.5	30	28			.638	32.5
	Brazilian	2	7	.697	34.9	325	68	1	4		206
41°	Natural							1	8	.513	27.2
	Natural	1	9	.569	29.6	2	25	2	18	.591	30.6
	Natural	2	15	.596	30.8	67	45	1	6	.681	34.3
30°	Saw Cut	2	11	.676	34.1	-6	31				44
	Brazilian	3	8	.824	39.5	204	103	1	2	.708	35.3
	Brazilian	11	44	.651	33.1	40	121	9	69	.620	31.8
Cumulative (All Cycles)	Natural	6	32	.680	34.1	20	48				126
	Saw Cut	5	15	.713	35.5	314	103	2	4	.649	33.0
	Brazilian										26

* Based on maximum shear stress.

[†] Tests run on previous study.

axis or fractured longitudinally in Brazilian tension. Artificial joints were approximately 2 inches in diameter by 4 inches long. Typical profiles of natural, saw-cut and Brazilian joints are shown in Figure 30.

Various load paths (Figure 31) were followed in the laboratory shear tests. The majority of tests were either direct shear (constant σ_n) or 30° and 45° proportional shear. Several $37\frac{1}{2}^\circ$, one 41° and one negative 45° proportional load paths were also run. The angles (30° , $37\frac{1}{2}^\circ$, 45°) of the proportional load paths were chosen to simulate the loading conditions in the *in situ*, triangular prism tests, where the natural joints were oriented at different fixed angles, α , relative to the prism axis. The angle α (Figure 32) fixes the relative amount of shear stress (τ) and normal stress (σ_n) applied to the joint as the pressure (P) is increased. From geometric constraints it follows that,

$$\cos \alpha = \frac{\tau}{P} \quad \text{and} \quad \sin \alpha = \frac{\sigma_n}{P}$$

$$\frac{\tau}{\sigma_n} = \frac{\cos \alpha}{\sin \alpha} = \frac{1}{\tan \alpha} \quad \text{or} \quad \tau = \frac{\sigma_n}{\tan \alpha}$$

and where $\alpha = 30^\circ$, $37\frac{1}{2}^\circ$ and 45° , then $\tau = 1.73 \sigma_n$, $1.3 \sigma_n$ and σ_n respectively. Thus, the laboratory proportional shear test directly simulates the load path in the field shear test. The laboratory and field tests do differ, however, in the amount of initial normal stress applied to the joint. The initial σ_n in the field is zero. However, in the laboratory shear test, initial σ_n is known and easily varied. Results from a typical laboratory 45° proportional shear test on a natural joint are shown in Figure 33.

Due to the differences in joint roughness, joint filling and actual joint contact area, particularly between natural and Brazilian joints,

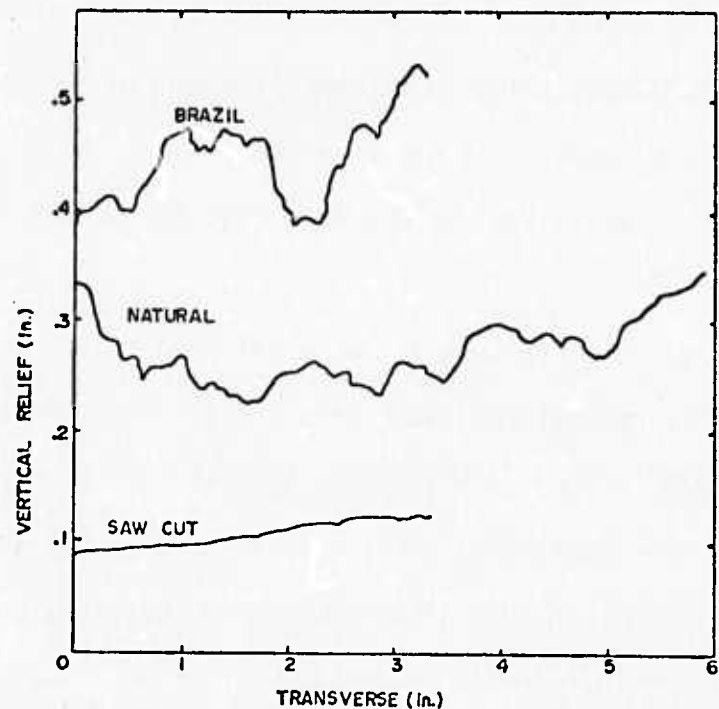


Figure 30. Typical profile of natural and artificial joints, Cedar City, Utah.

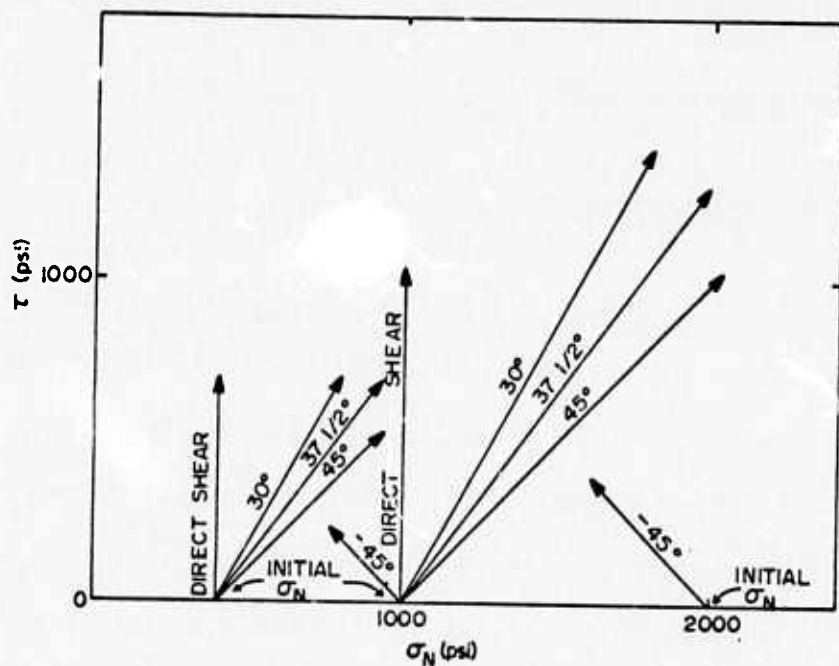


Figure 31. Direct shear and proportional shear load paths.

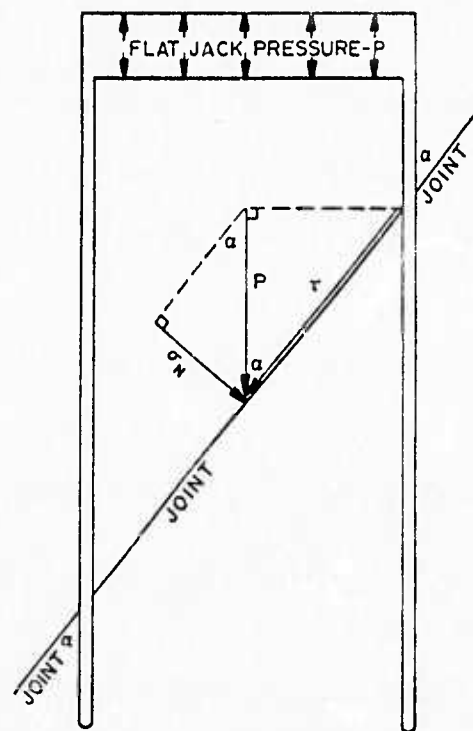


Figure 32. Field specimen joint orientation.

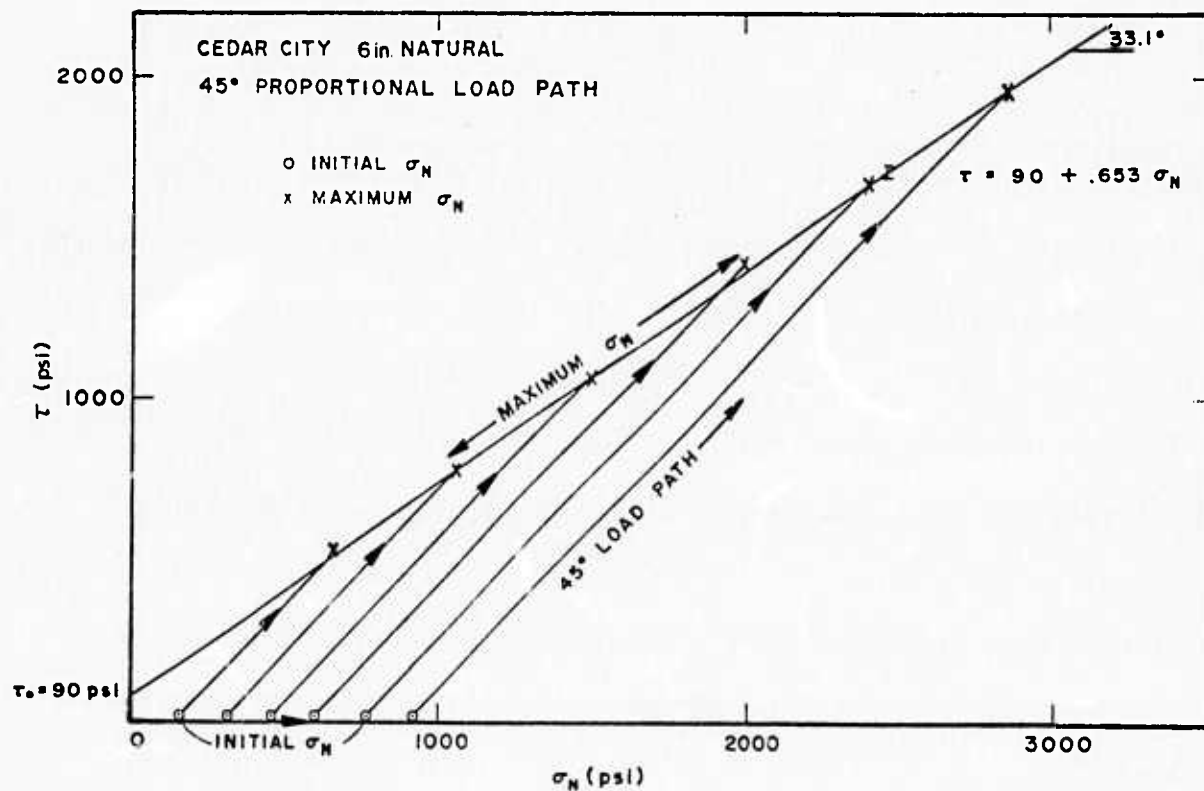


Figure 33. Shear stress-normal stress curve for 45° proportional load path, Cedar City.

the test results show variable data scatter between different joints tested. Therefore, test results from individual tests have been grouped and analyzed according to (1) joint type (natural, saw-cut, Brazilian) and (2) load path. A least square straight line fit and the standard deviation of individual data points from the straight line (Figures 34, 35 and 36) have been computed for each group of data. The bar on the straight line is the standard deviation of shear stress (τ) and the number in parenthesis near the bar is the number of data points represented by the straight line fit. The equation of the straight line is $\tau = \tau_0 + \mu \sigma_n$ where τ_0 is the intercept and represents joint cohesion and μ is the coefficient of friction. Values of τ_0 and μ as well as friction angle, ϕ , and standard deviation, τ_{dev} , are presented in Table I.

The relative shape and magnitude of typical shear stress-shear displacement curves (Figures 37 and 38) for natural and saw-cut joints sheared under direct, 30° and 45° loading cycles can be seen. The initial and the maximum σ_n corresponding to the maximum τ and the sequence of cycling are noted in the graphs. The shear displacements are shown to start at zero displacement for clarity. However, each cycle is sheared at progressively larger displacements along the joint as shown in Figure 39. The shear stiffness or slope of the curves generally increases at higher σ_n . Also, specimens with natural joints shear to a residual shear stress lower than the maximum shear stress, while saw-cut specimens shear to a residual stress nearly equal to the maximum shear stress.

The magnitude of maximum shear stress is reduced by prior loading history. Figure 40 is an example of a natural joint sheared to approximately 0.5-inch displacement (8% of total length) and then repositioned

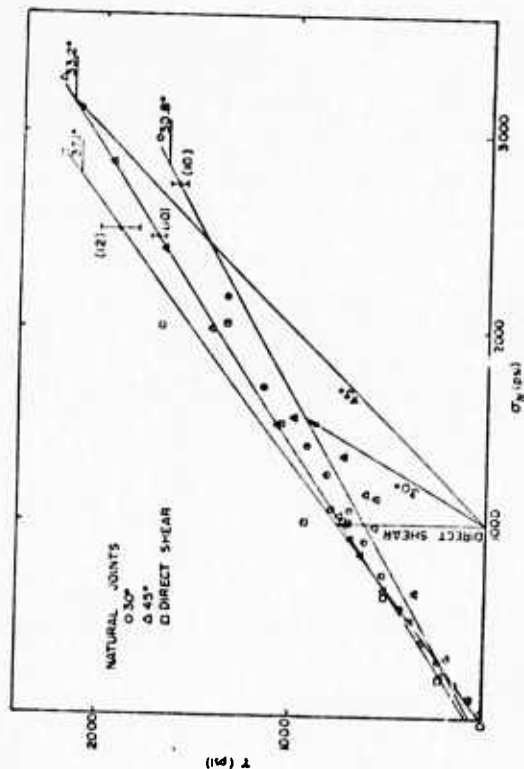


Figure 34. Data scatter and statistical fit of τ vs σ_n curves for natural joints sheared under various load paths, Cedar City.

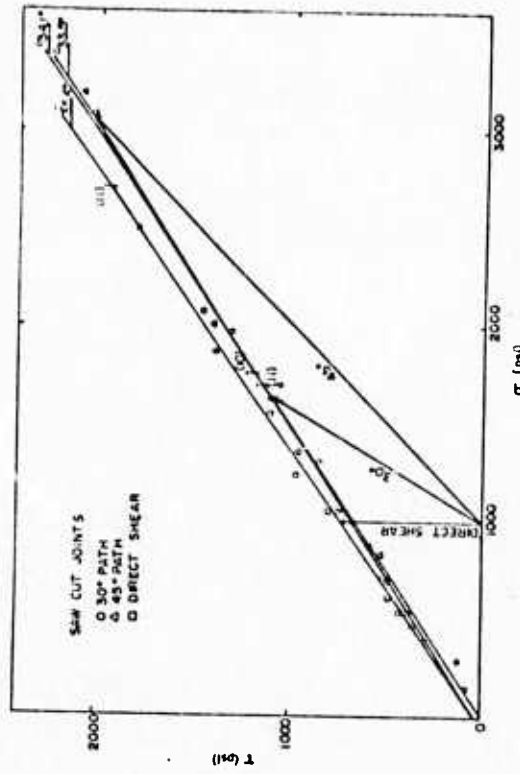


Figure 35. Data scatter and statistical fit of τ vs σ_n curves for saw-cut joints sheared under various load paths, Cedar City.

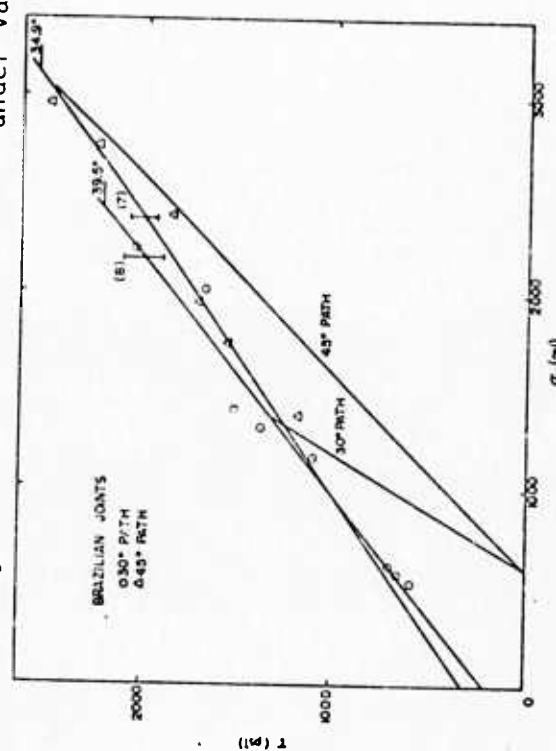
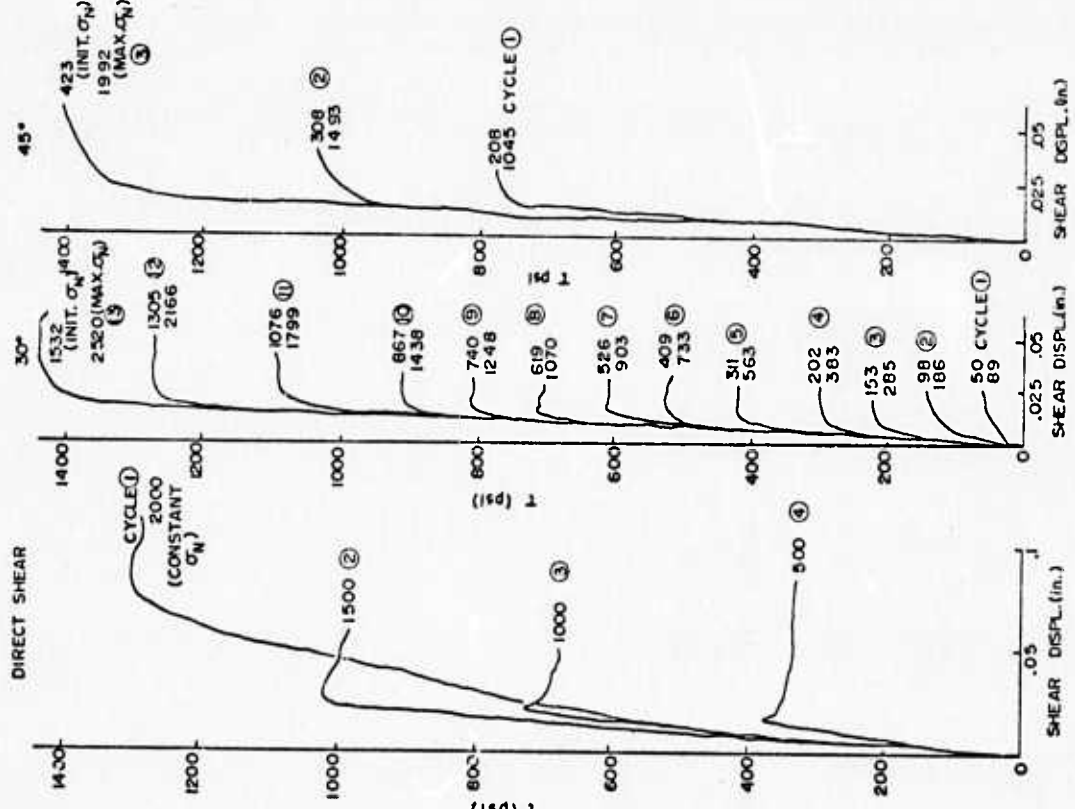


Figure 36. Data scatter and statistical fit of τ vs σ_n curves for Brazilian joints sheared under various load paths, Cedar City.



46

Figure 37. Shear stress displacement curves for natural joints (Cedar City) sheared at various normal stresses and 30°, 45° and direct shear load paths.

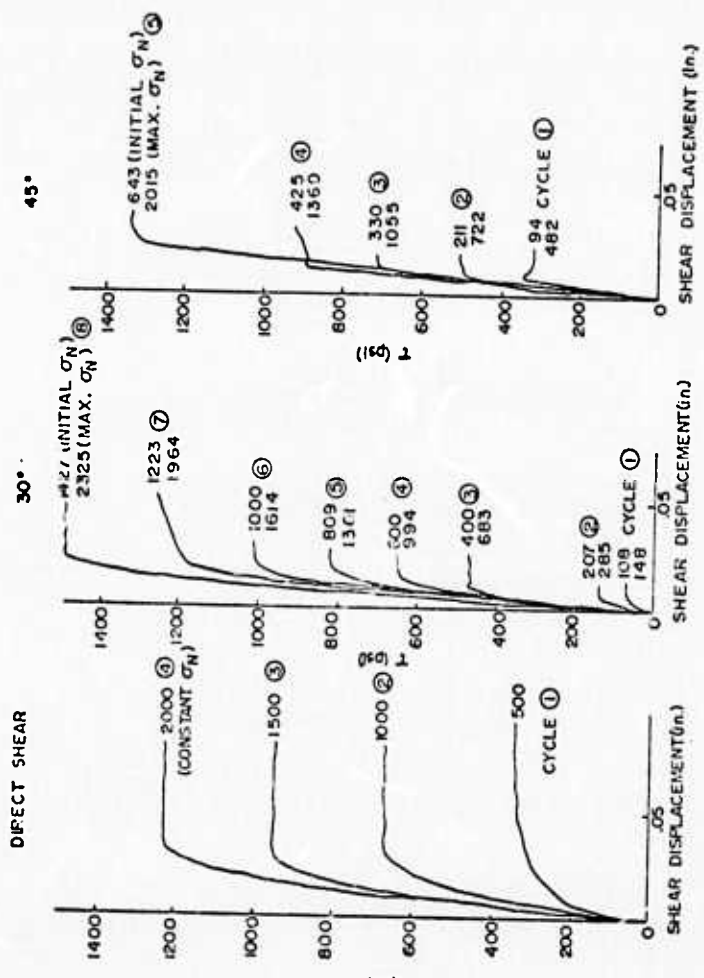


Figure 38. Shear stress displacement curves for saw-cut joints (Cedar City) sheared at various normal stresses and 30°, 45° and direct shear load paths.

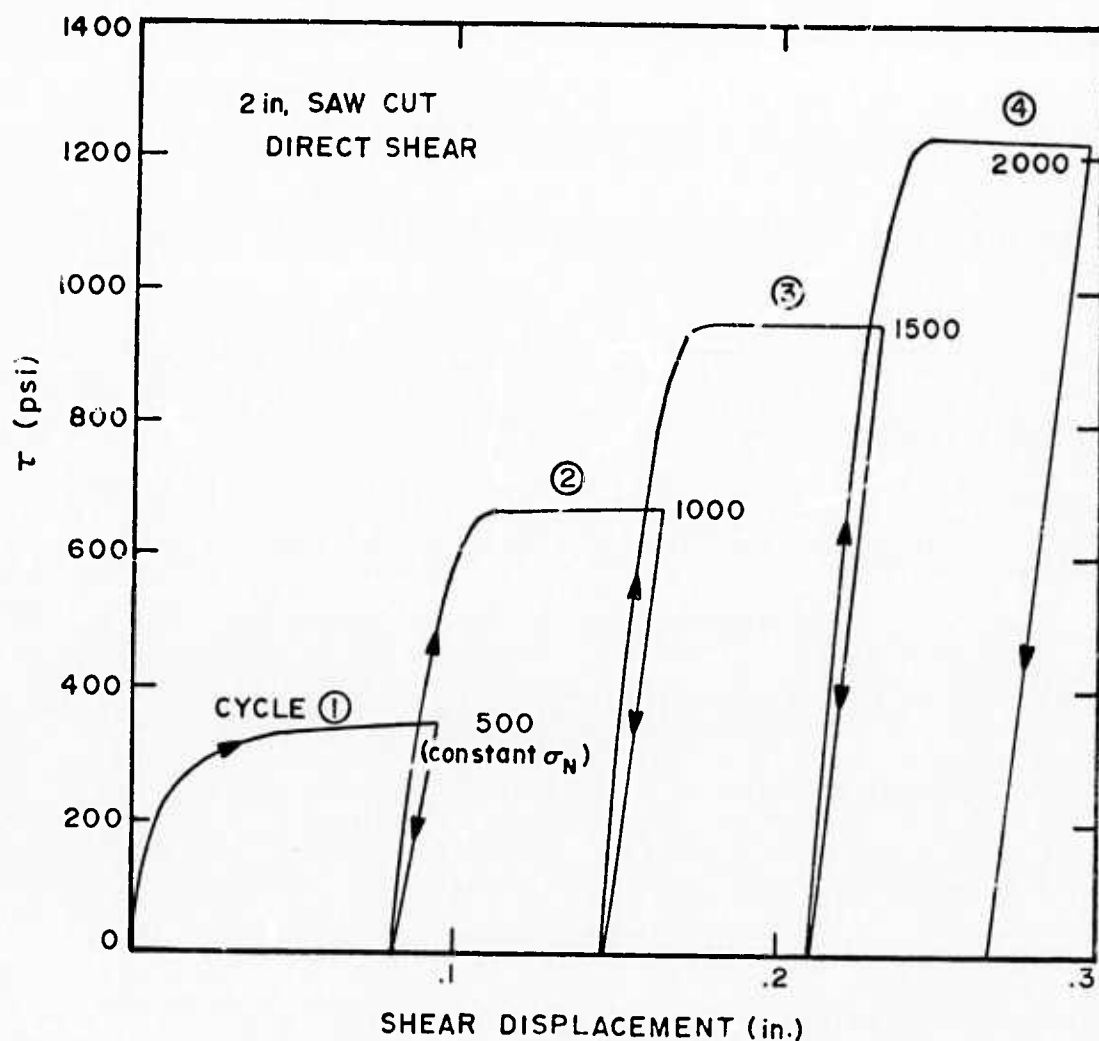


Figure 39. Shear stress displacement for a saw-cut joint cycled at different normal stresses, Cedar City.

and sheared again under the same load conditions. The friction angle from first to second shearing was reduced (Figure 41). The effect of repositioning on the friction angle for all direct shear tests on natural joints (Figure 42) is also shown. The friction angle of repositioned specimens sheared to "large" displacements is obviously lower than virgin specimens loaded under the same conditions. However, the effect of cycling a virgin joint under various load conditions to "small" shear displacements does not appear to change joint frictional properties significantly. Two series of direct-shear tests were conducted (Figure 42). In one series, individual virgin specimens were sheared once only and to large displacements; in the second series, virgin specimens were sheared several times each at different normal stress and to "small" shear displacements. The resulting friction envelopes are essentially the same (37.1° and 36.4°) and fell well within one standard deviation of each other.

The influence of joint roughness and contact area on the friction angle was investigated. A cumulative graph (Figure 43) of tests which include all loading cycles and load paths run on natural, saw-cut and Brazilian specimens illustrates the variation of friction angle for the three joint surfaces. Also, differences in friction angle between the three surfaces for 30° and 45° load paths (Figures 44 and 45) are shown. The frictional properties of a given joint depend on the resultant effects of both surface roughness and contact area. This observation is illustrated schematically in Figure 46. From joint profiles (Figure 30) the relative surface roughness is apparent, and the relative contact area can be seen by inspecting the surface gouge after shearing takes place. A striking example of a low contact area is shown (Figure 47)

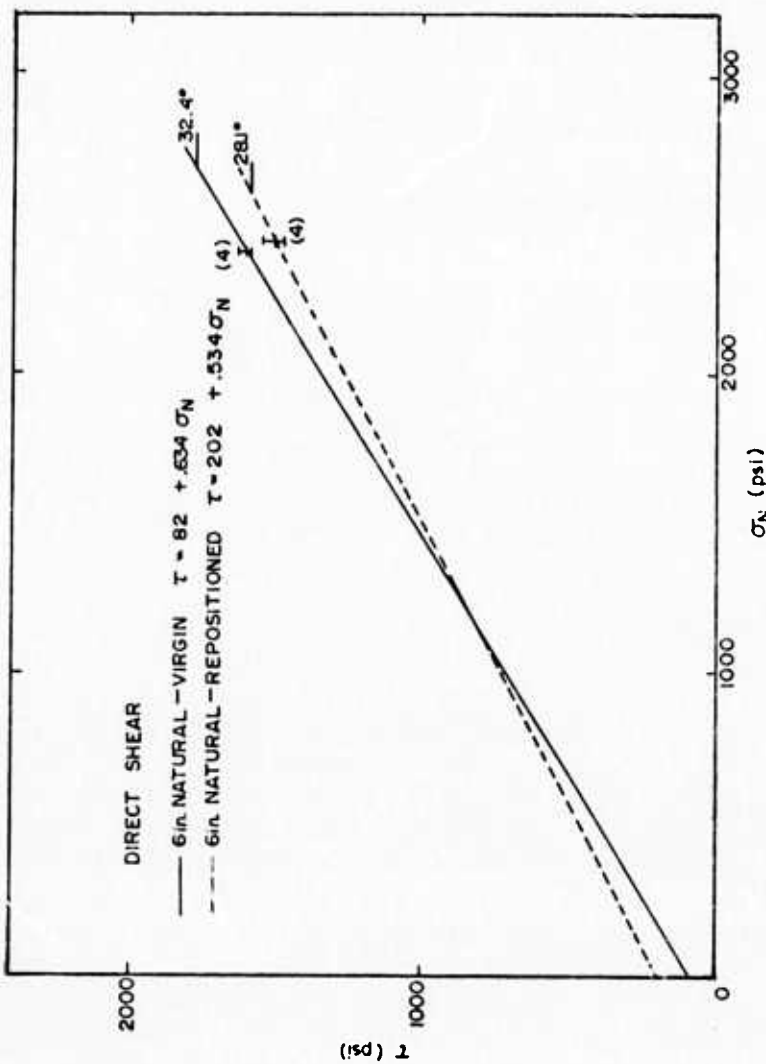


Figure 41. Shear stress-normal stress for a single virgin and repositioned natural joint, Cedar City.

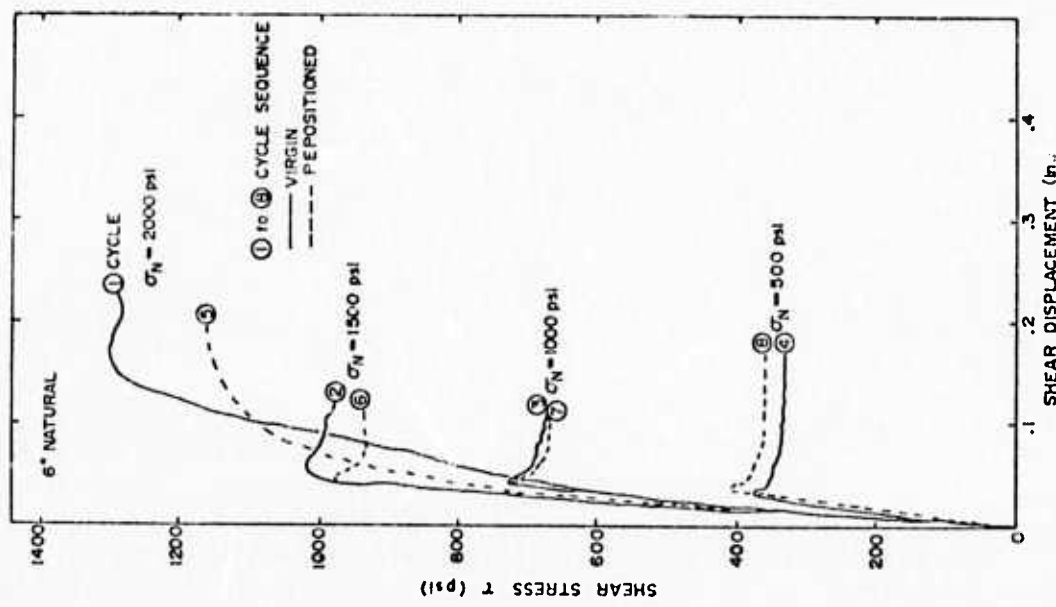


Figure 40. Shear stress-displacement for a single virgin and repositioned natural joint, Cedar City.

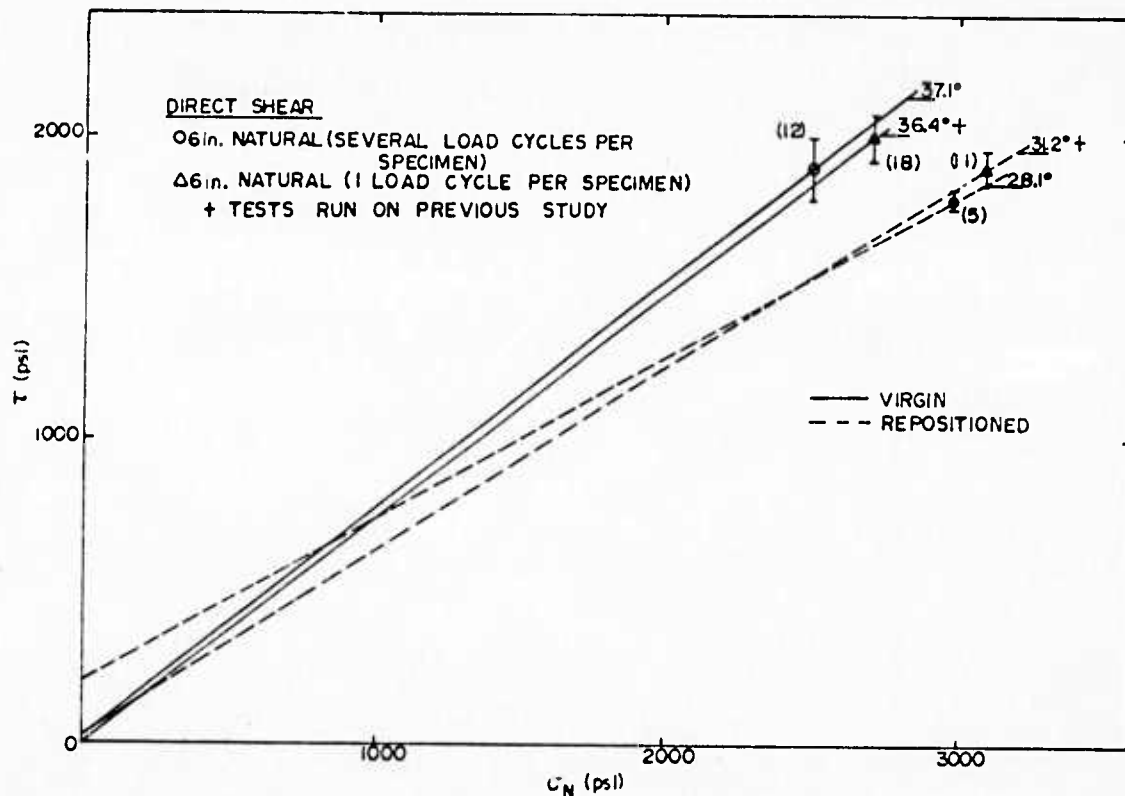


Figure 42. Shear stress-normal stress for natural joints (Cedar City) shear under either one or several direct shear load cycles.

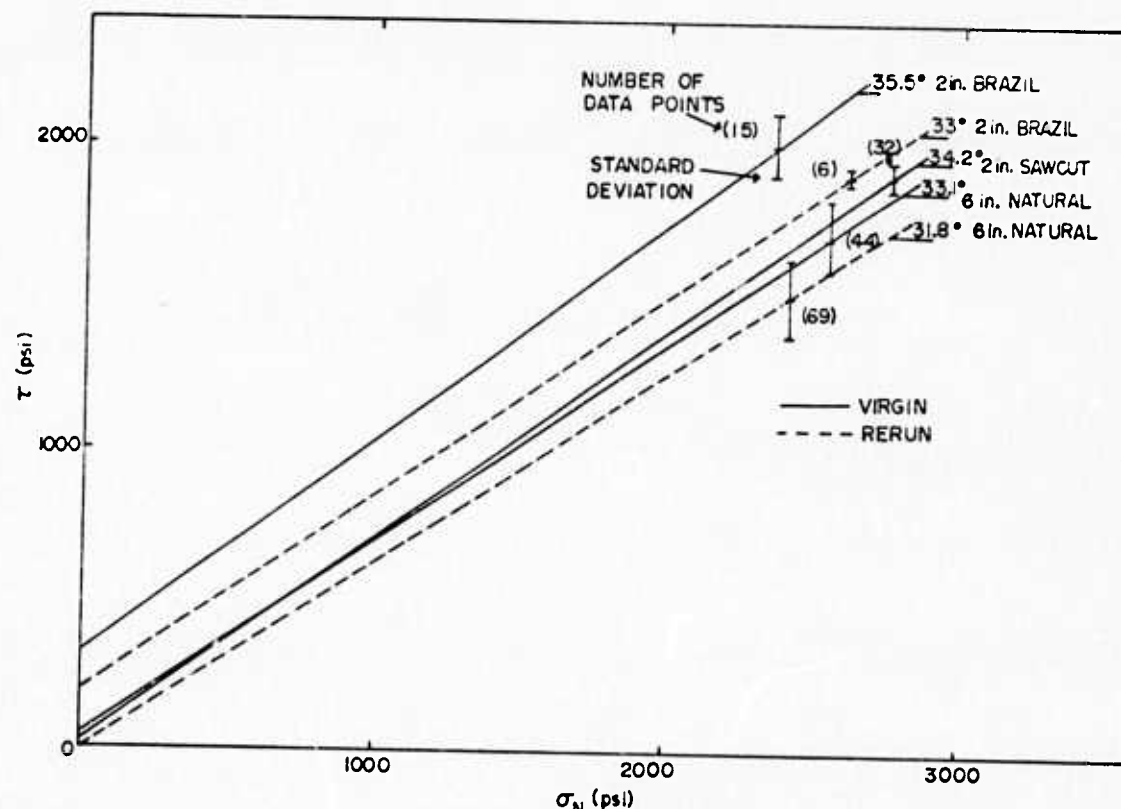


Figure 43. Cumulative shear stress-normal stress for natural, saw-cut and Brazilian joints (Cedar City) sheared under various load paths.

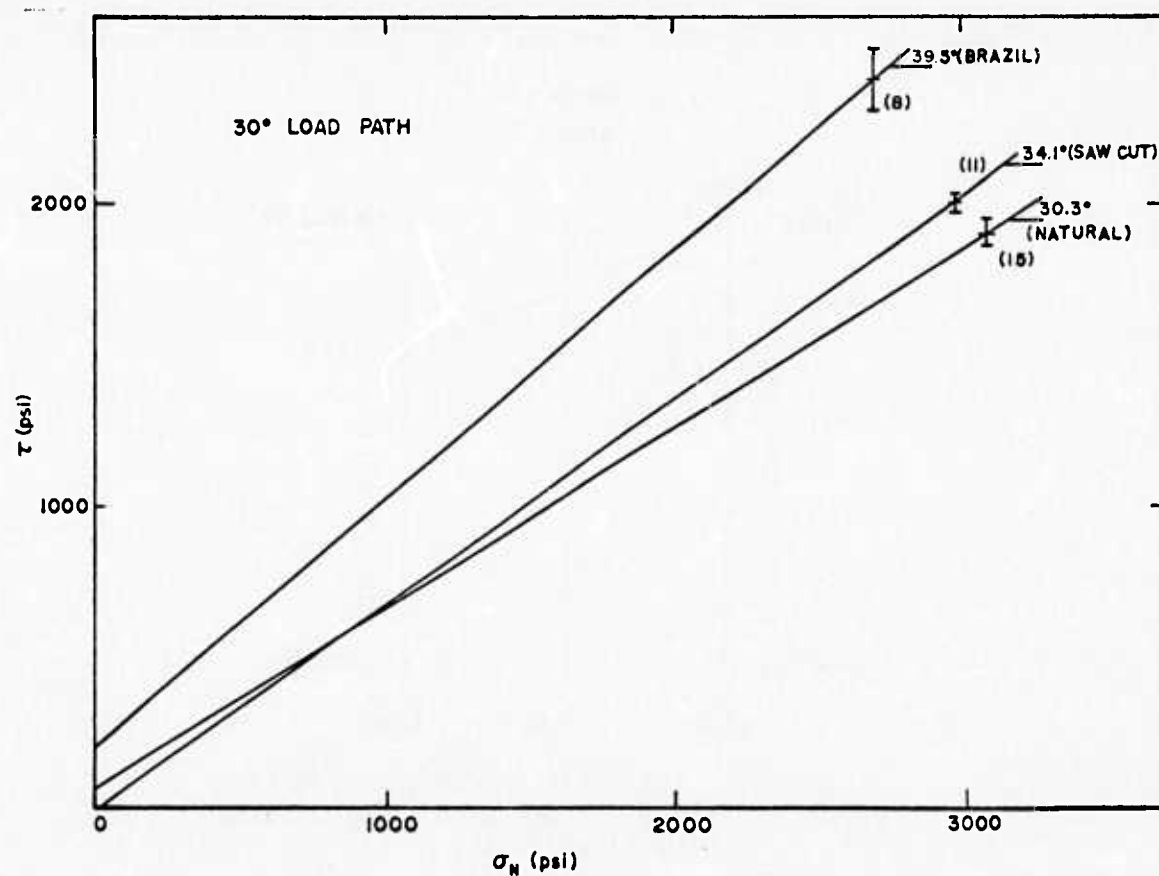


Figure 44. Shear stress-normal stress for natural, saw-cut and Brazilian joints (Cedar City) sheared under 30° load path.

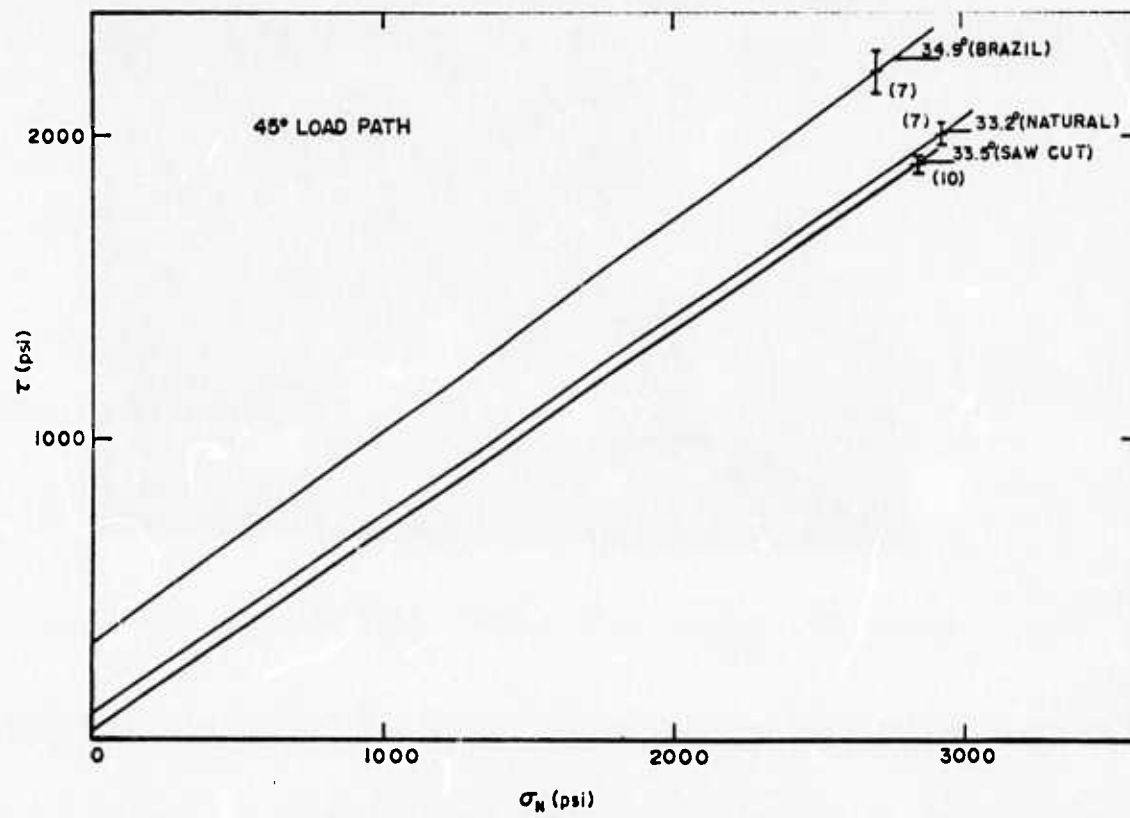


Figure 45. Shear stress-normal stress for natural, saw-cut and Brazilian joints (Cedar City) sheared under 45° load path.

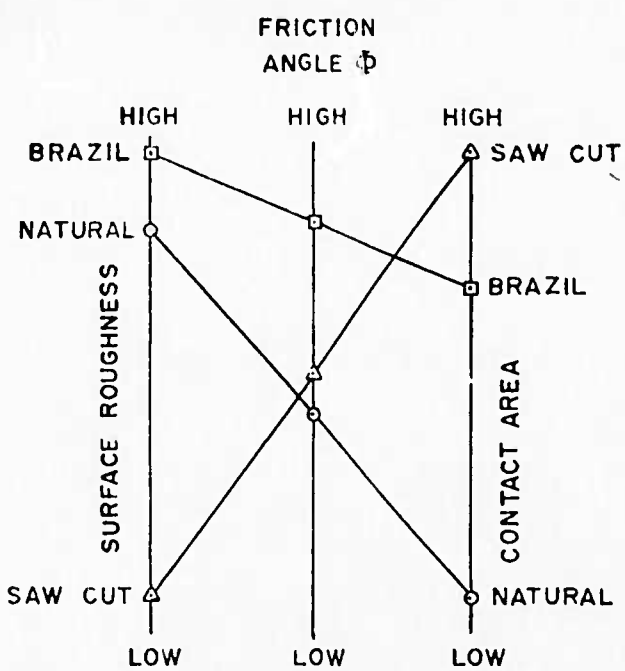


Figure 46. Schematic of surface roughness and contact area effects versus friction angle.

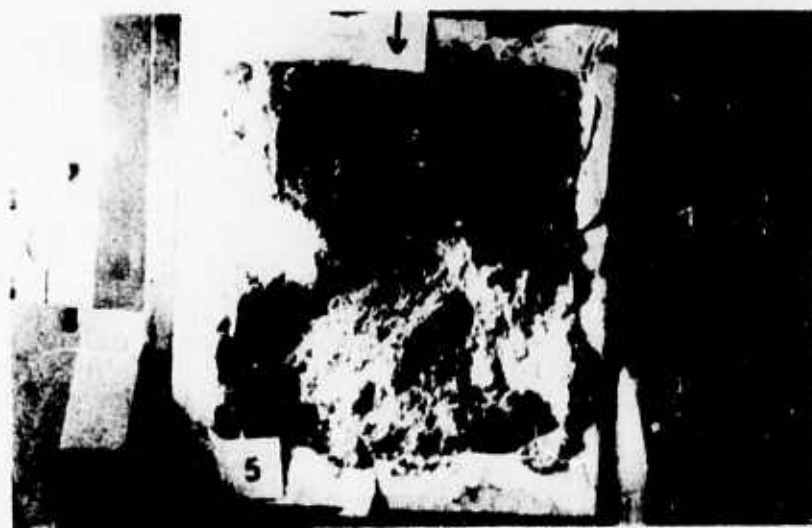


Figure 47. Natural joint (Cedar City) with low contact area.

where an irregular natural joint partially filled with soil was sheared. The lighter areas of the photograph are gouged or contact points, while the dark area was untouched. The contact area of the specimen was approximately 30 percent. The resulting friction angle was 28.1° compared with 33° for all other similar load paths on natural joints.

The effect of load paths (constant normal stress and 30° and 45° proportional stress) on friction angle for saw-cut and natural joints was also investigated. Results for saw-cut specimens do not conclusively show path dependence; however, there is a slight decrease in friction angle from direct shear to 30° and 45° proportional loading tests (Figure 48). For a natural joint, however, a more striking difference in friction angle occurs for different load paths. Even though the variability in data for natural joints is large compared to saw-cut joints, there appears to be a definite trend in the data which indicate a load-path effect, especially for the 30° and $37\frac{1}{2}^\circ$ paths (Figure 49).

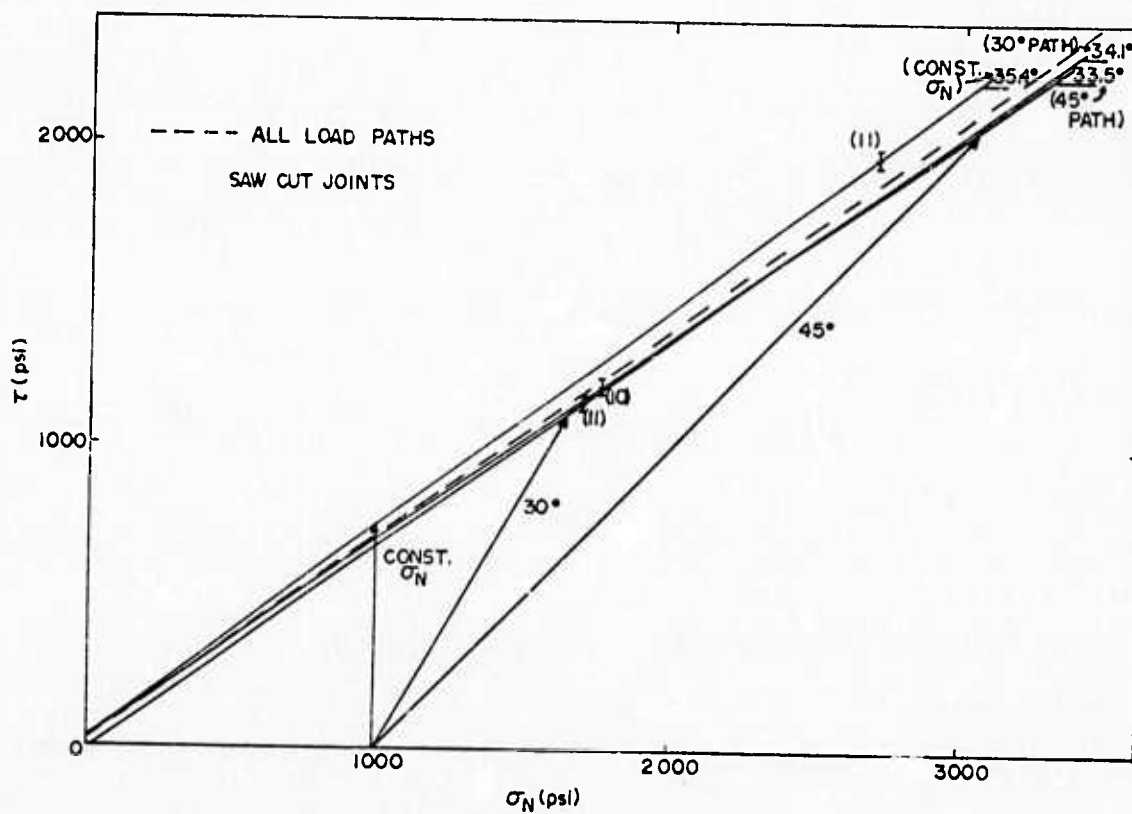


Figure 48. Saw-cut joints (Cedar City) sheared under various load paths.

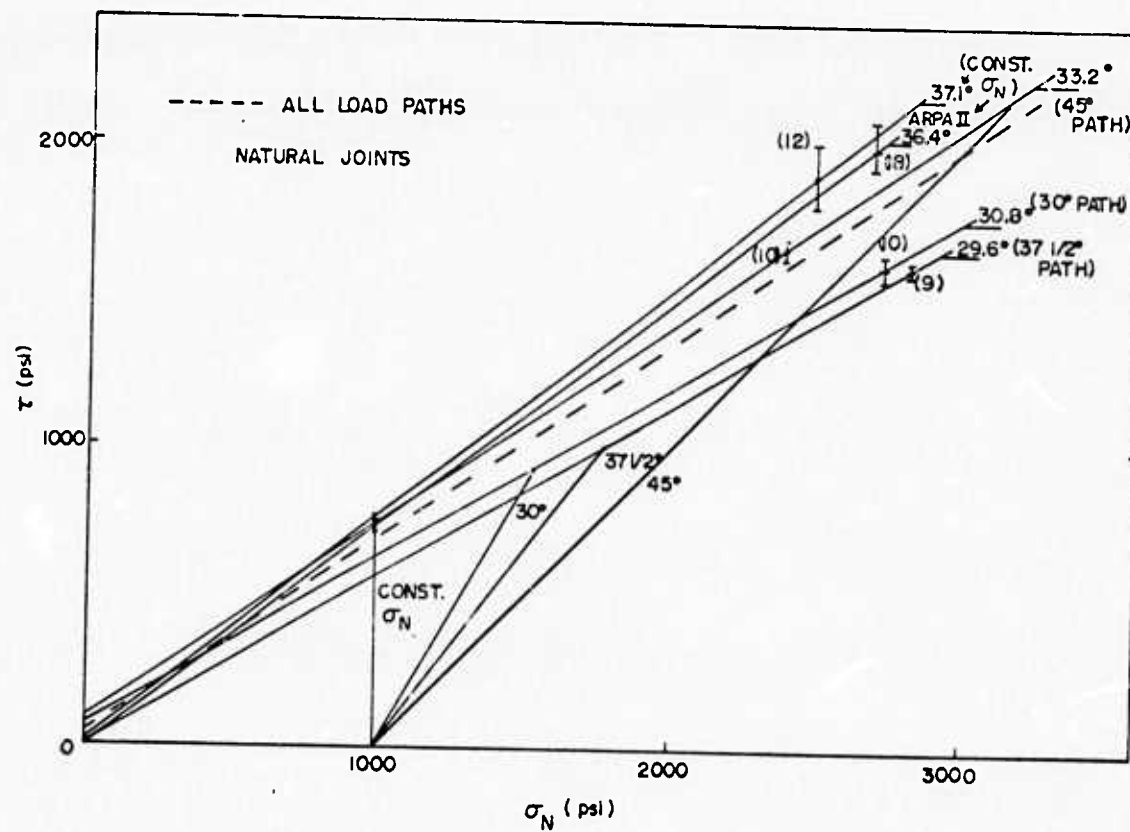


Figure 49. Natural joints (Cedar City) sheared under various load paths.

SECTION VII

DISCUSSION

To date, 46 *in situ* tests (24 intact and 22 jointed specimens) have been conducted in a variety of rock types including granite, sandstone, amphibolite and chloritic schist. Specimens have been cut out and tested in terrain ranging from horizontal outcrops to nearly vertical tunnel walls. Specimens have ranged from effective diameters of 6 to 50 inches. Tests on specimens with a single joint have been conducted on surface areas ranging from 22 square inches to 5.5 square feet.

The length of time involved in testing an *in situ* specimen, including specimen preparation, flatjack emplacement, instrumentation and actual testing ranges from 3 days for a 1 by 2 foot specimen to 5 days for a 3 by 6 foot specimen. The difference in the time periods reflects the time required for actual excavation of the specimen. During the instrumentation and testing of one specimen a second specimen can be prepared thereby decreasing the total time required at a test site.

Stress-strain data for intact rock (Figure 50) illustrates the data scatter from a single test. This data spread is similar in magnitude to that from laboratory tests with a comparable number and distribution of strain gages. Modulus and Poisson's ratio data are obtained from gages located in the center of the specimen.

The *in situ* shear test differs from a direct shear test in that a direct shear specimen is sheared at a predetermined stress applied normal to the discontinuity, while the normal stress on the joint of

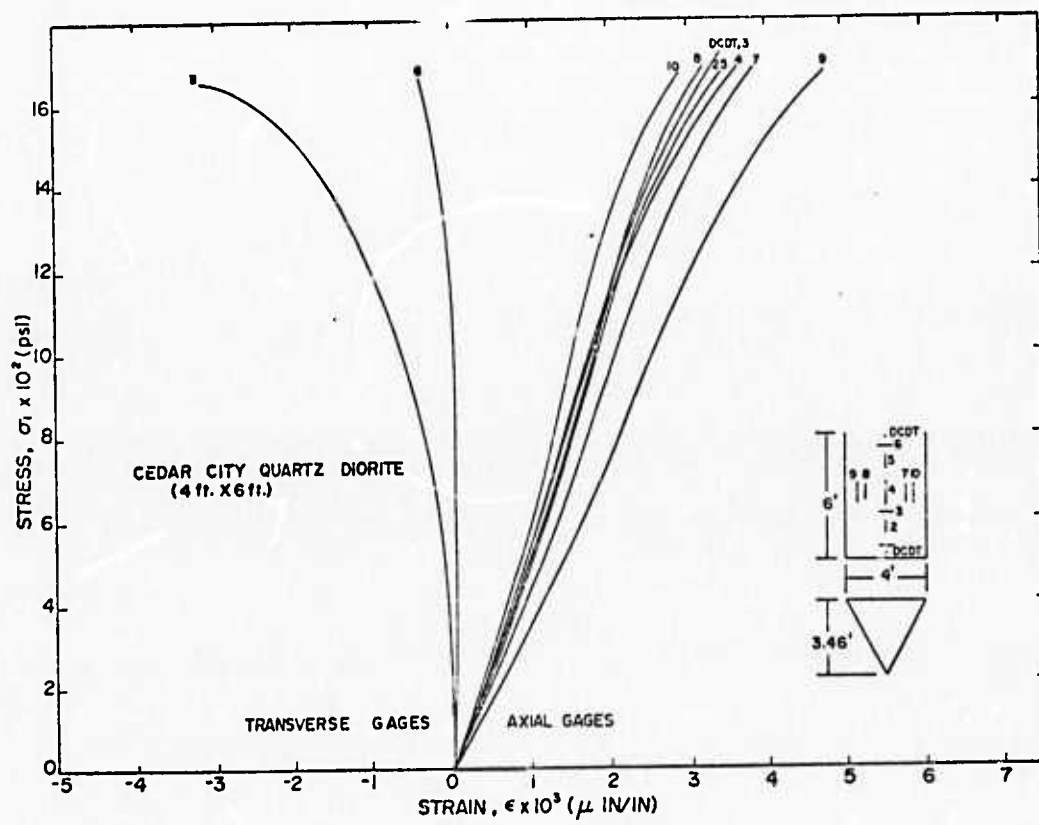


Figure 50. Typical stress strain data.

our *in situ* specimen is continually increasing as the specimen is loaded because of the fixed joint angle. Thus, the loading paths differ for the two tests. In either *in situ* or laboratory direct shear tests, the friction envelope is developed by shearing a specimen(s) at a series of normal stresses. *In situ* the envelope is developed by conducting a sequence of tests with the joint at different angles to the loading axis.

The shape of the shear stress-displacement curve is dictated by the character of the joint (Figure 51). As fresh, intact joints (curve 1) are sheared, there is a rapid decrease in shear strength from an initial shear strength (τ_i) to a residual shear strength (τ_r). In contrast, joints with filling material such as calcite or clay (curve 2) have curves whose τ_i and τ_r are nearly the same and whose shear stiffness is also significantly lower. The shear stiffness is defined as the slope of the shear-stress-displacement curve.

Several test programs have been conducted by Terra Tek to determine material property data that will be useful in formulating realistic models for rock mass response to static and dynamic loads. These include: (1) the effect of specimen size on strength and deformation of "intact" rock.² (2) the effect of joint surface area on frictional properties (coefficient of friction, shear stiffness, normal stiffness) of natural joints, (3) effect of joint orientation on shear strength, (4) effects of joint filling material in frictional properties, (5) a comparison of frictional properties determined by our *in situ* technique and laboratory direct shear tests, and (6) a comparison of deformation of singly- and multiply-jointed specimens.

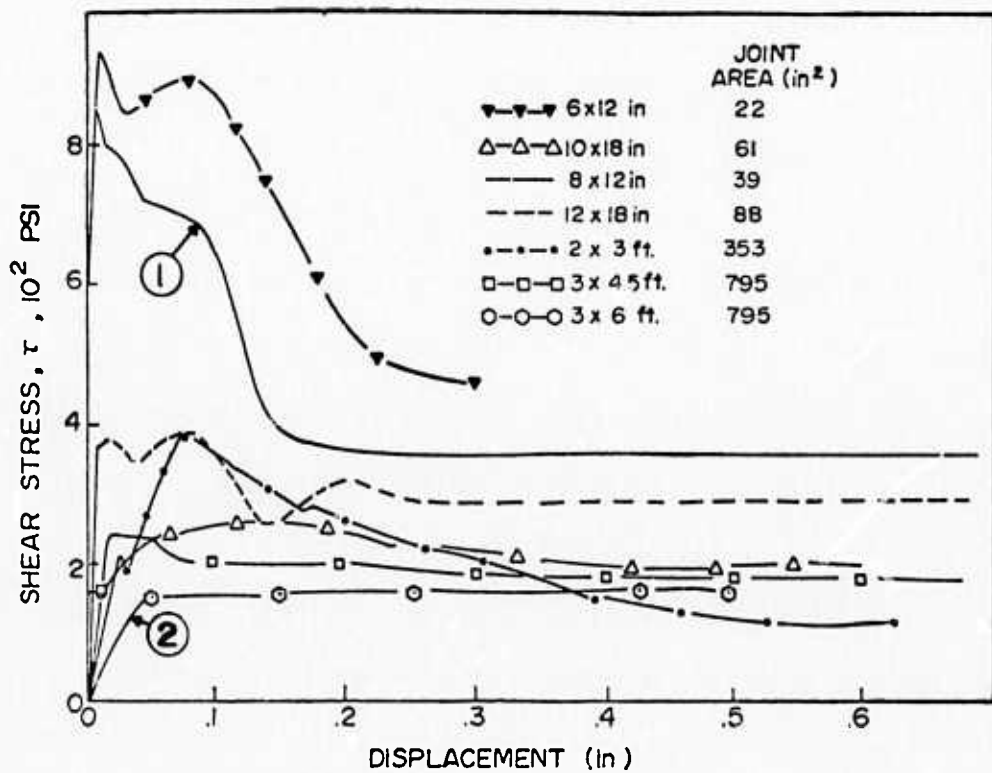


Figure 51. Shear stress versus displacement for joints with different surface areas. All specimens had a single joint oriented 45° to axis of loading.

To evaluate the use of the Terra Tek technique for testing *in situ* intact and jointed rock, several factors should be considered. (1) The technique is limited to rock masses competent enough to allow sample preparation without significant disturbance. (2) Only exposed rock can be tested. (3) The load is static and rate effects must be extrapolated if dynamic properties are wanted. (4) Since the rock mass itself acts as a reaction frame for loading the triangular prism, the competence of rock around the specimen must be considered to avoid rock failure other than within the specimen. (5) Since the ratio of normal stress to shear stress applied to a jointed specimen is fixed by the orientation of the joint with prism axis, two or more tests are required to obtain a friction envelope.

In spite of the above constraints and limitations, we feel that our technique has advantages and features which make it a valuable tool for measuring the strength and frictional properties of rock *in situ*. (1) Compared to conventional laboratory specimen sizes, relatively large volumes of rock can be tested which contain fractures and discontinuities representative of rock mass properties. (2) Large joint areas can be sheared to large displacements, so that frictional properties can be measured on natural joints where wave length and amplitude is significant. (3) The specimen is a homogeneously-stressed solid. (4) Tests have been successfully conducted using this test technique for intact and jointed specimens in a variety of rock types, over a significant range of specimen sizes with the logistical constraints typical of construction sites or exploratory tunnels.

Tests have been conducted at two Bureau of Reclamation dam sites and the Mixed Company test site at or as near as possible to locations

where *in situ* direct shear, uniaxial jacking and radial jacking tests were previously conducted. The purpose of conducting tests at the dam sites was to determine the potential of this approach as a practical measuring technique and to compare our test results with the previously obtained results from other shear and deformation tests. The specimens have been prepared and successfully tested under constraints at such sites. The tests were conducted at the Mixed Company site to measure strength and deformation *in situ* and to determine the effect of specimen size.

Size Effects

This and other studies^{22,23,24} have shown that both the strength and deformation moduli (stiffness) of rock masses is considerably less than small intact laboratory samples. The magnitude of difference between rock mass and laboratory properties has been shown to be up to a factor of 10. These differences have been attributed to the number, character and orientation of discontinuities within the rock mass and to size effects in "intact" blocks within the rock mass.

Our studies have been conducted on both intact and jointed specimens ranging in size from 3/4-inch to 50-inches in diameter. The tests were carried out in both the laboratory and *in situ*. An intact specimen is simply defined as a rock sample without discernable joints or fractures on the exposed surfaces. Results from tests on two rock types, diorite and sandstone, indicate that there is a significant decrease in strength, ranging from a factor of 2 to a factor of 4, with increasing specimen size for intact rock (Figure 52). Beyond an apparent critical size, the

strength remained constant. This critical size has important considerations with respect to obtaining rock mass properties. The effect of specimen size on the compressive strength of intact samples has been debated. Several authors have found no size effect for samples up to 6 inches in diameter.^{25,26} Some authors^{27,28} found relatively small size effects (up to 25 percent) for small samples over a limited range of sizes (Figure 53). Huck²⁹ found a decrease in strength by a factor of two on samples of granite up to 32 inches in diameter. To date, these samples are the largest tested in the laboratory. Large-scale size effects have been noted for *in situ* coal samples³⁰ (Figure 53).

Calculations of the response of large rock masses to static or dynamic loads depend to a large extent on measurements made on specimens in the laboratory and *in situ* studies such as we describe here. In either case, the specimen is often much smaller than the prototype and so appropriate scaling of data is of paramount importance. Studies of the effect of size on material properties have been directed primarily towards predicting the strength of large bodies from the strength of small models and the effect of size on modulus and friction has received little attention. Weibull's theory for the effect of size on strength has received acceptance in engineering circles and is widely used for predicting strength of manufactured parts. The fundamental basis of the theory, that the strength of a body is governed by the presence of flaws, is appropriate for rocks where the relatively low strength is generally attributed to the presence of cracks. Weibull assumes that the weakest element, i.e., the largest flaw, determines the strength of a sample. A certain "underlying distribution" of flaw sizes is assumed to be characteristic of a given material, independent of the size of the sample.

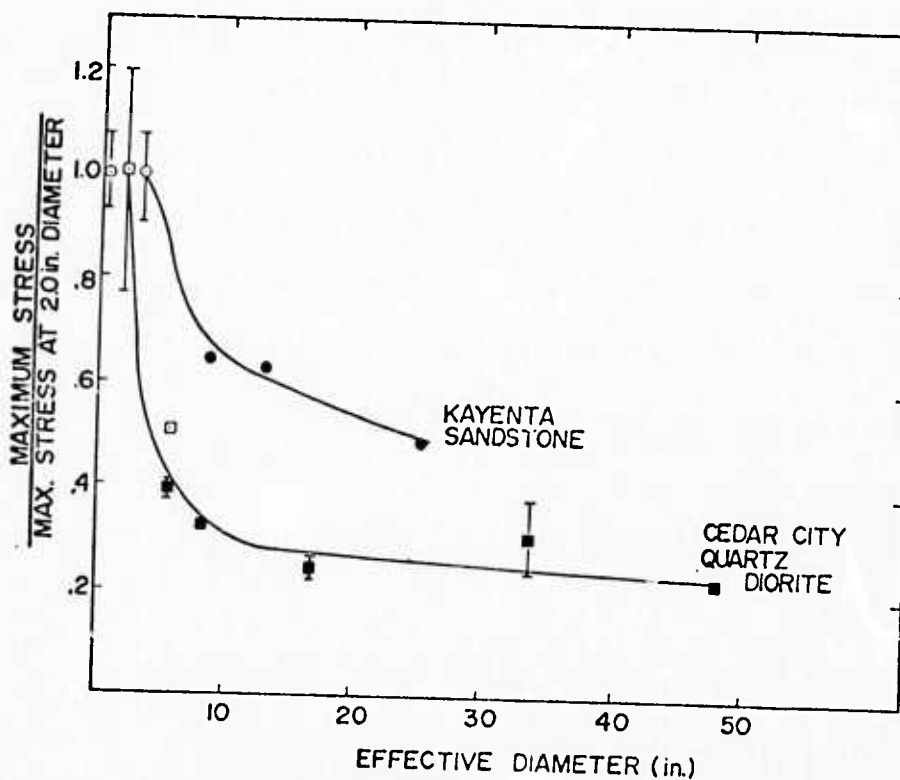


Figure 52. The decrease in strength as a function of specimen size for diorite and sandstone.

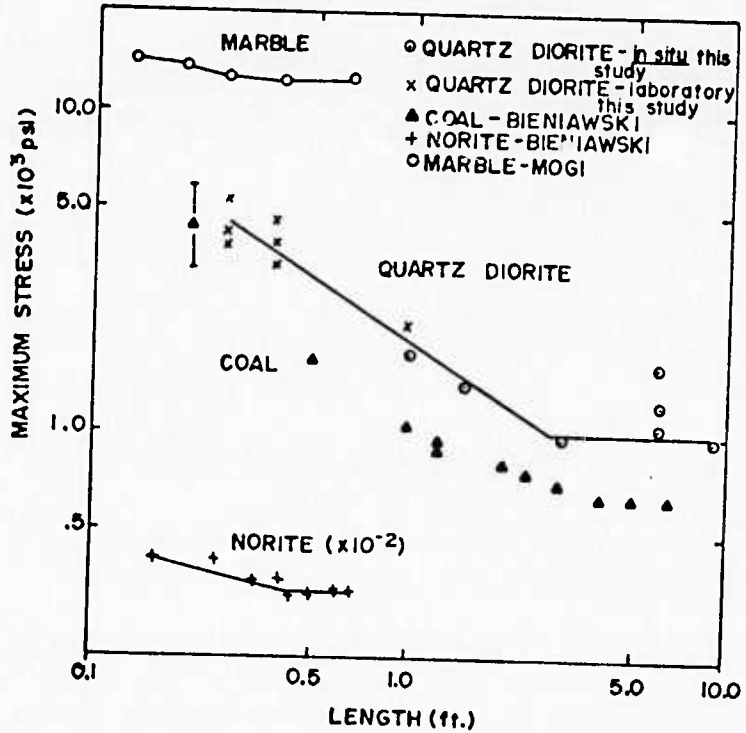


Figure 53. Size effects for a variety of rock types.

Large samples therefore are usually weaker than small ones because of the greater probability of finding a large flaw among the greater number of flaws present in a large sample.

Whether the size effect we find in Kayenta sandstone and Cedar City quartz diorite (Figure 52) is, in fact, explained by Weibull's theory is open to question. In the first place Weibull assumes that strength is limited by the single largest crack, whereas fracture of rock in compression involves the growth and coalescence of many cracks. Micro-cracks are known to form randomly over a wide range of stresses up to 80 to 90 percent of failure strength at which time they begin to initiate and grow in a zone along which ultimate failure occurs. A single crack somewhat larger than the general population probably has little influence on the compressive strength of our samples.

Also, we cannot be sure that the underlying distribution of flaw sizes is independent of the size of our specimens as assumed in the theory. It is entirely possible that larger cracks are present in our large specimens than in the small ones. An intact sample cannot contain a flaw larger than the sample itself, after all. The low strength of the large samples described in Figure 52 may be due simply to the presence of (relatively) very large cracks; however, this explanation is entirely speculative until someone determines the entire spectrum of flaw sizes present in large rock masses.

The possibility exists that the size effect measured in our study and in others is due to some factor entirely unrelated to the flaws which are present. The strength of a sample of quartz diorite *in situ* was found in another study² to be about the same as a sample of the same size measured in the laboratory, so the size effect in Figure 52 does not

appear to be due to some inherent difference between our laboratory and *in situ* testing techniques. Stress gradients have also been suggested as a possible cause of size effect, with small samples, where a relatively small volume of material is subjected to high stress, being stronger than large samples. The length/diameter ratio of our samples is sufficiently large that stress concentration due to end constraint has a small effect on stresses in the section where fracture occurs. Stress gradients are, therefore, probably too small to account for the large effect exhibited by the data in Figure 52. The explanation for the effect of size upon the strength of rock in compression is subtle, judging by the lack of a generally accepted theory, and a more comprehensive investigation is needed.

The shear strength of natural joints was tested over a wide range of surface areas from 20 to 1000 inches.² Again, a size effect was noted, with the shear strength decreasing with increasing surface area (Figure 54). The size effect that we noted over a large range of surface areas of natural joints is attributed to a contact area effect. It is apparent from post-test examination of sheared joints that the contact area may be as low as 10 to 20 percent, depending on the wave length and amplitude of the asperities and the secondary modification of the joint. The stress applied to the joint during the loading phase is thus distributed only over the contact area so that the "real" shear stress is considerably greater than the stress calculated from the total area of the joint. This leads to the size effect for larger surface areas with lower contact area. The effect of contact area on shear strength has also been shown for laboratory specimens. This size effect would disappear if the contact area and relative roughness remained constant for all specimen

sizes. The effect would also diminish at high normal stresses for relatively soft material. The decrease in shear strength with size also appears to asymptotically approach a limiting value related to the wavelength and amplitude of the joint under consideration.

Deformation and Strength

The *in situ* modulus is a parameter required to calculate the global response of a rock mass. Our previous studies³³ have shown that there is no discernable size effect with respect to the modulus of intact samples. However, the modulus of *in situ* jointed rock has been shown to be considerably less than modulus data obtained from intact specimens.^{22,24} In our study the average intact modulus of Cedar City quartz diorite obtained from field samples was $.64 \times 10^6$ psi while that of rocks with multiple joints was $.12 \times 10^6$; a decrease of almost a factor of 5. Recent studies in granite using a Goodman jack to obtain deformation modulus indicated that the ratio of laboratory to *in situ* modulus ranged from 9.8 to 7.2 for 3000 and 9000 psi stress levels, respectively, and that the ratio at a given stress level also varied depending on the frequency and orientation of the joints.³⁴ The contribution of joint(s) to the total deformation depends on the initial apertures of the joints and loading state. Biaxial and uniaxial loading tests on a large *in situ* cube of granite illustrates these points.³⁵ In biaxial loading the contribution at a stress level of 500 psi of the individual joints ($D_4+D_5+D_6$) to the total deformation is approximately equivalent to the deformation of the intact rock (S_1) which contained extensive small fractures (Figure 55). The contributions to the total deformation of individual joints also varies. At low stress the joint contribution is significantly

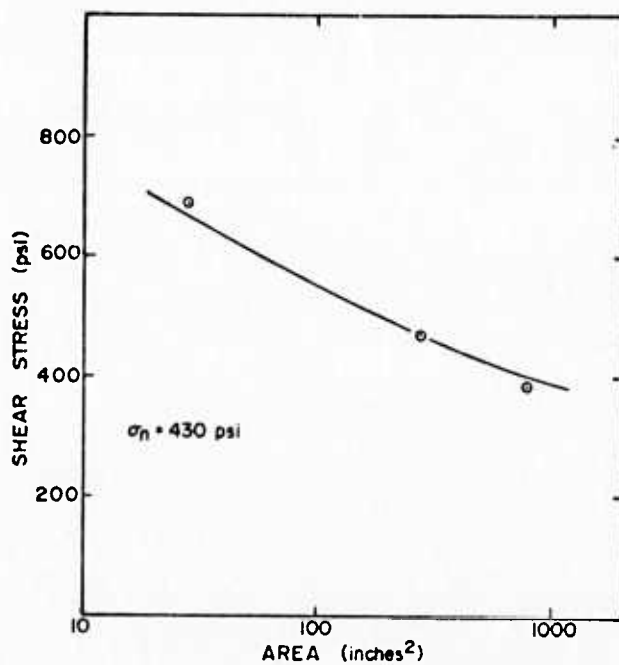


Figure 54. Maximum shear strength as a function of joint area. Specimens have a single joint.

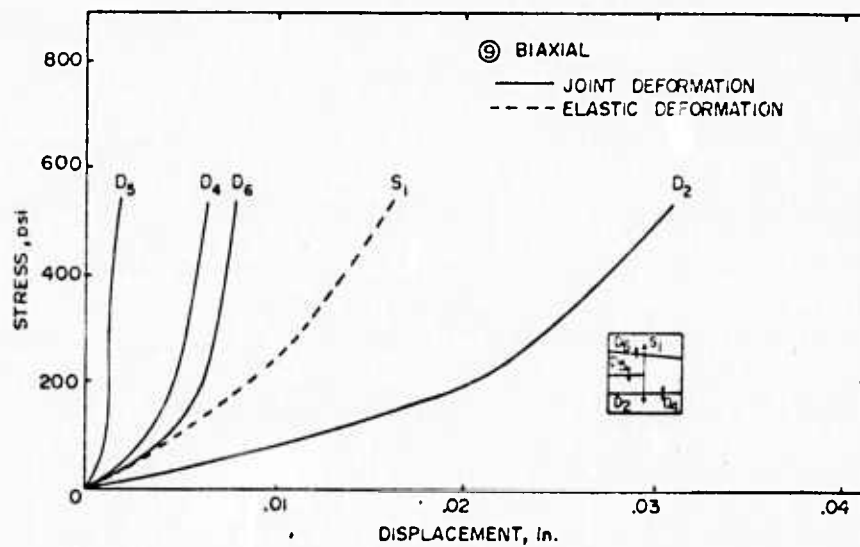


Figure 55. Stress-displacement diagram showing the contribution of closure of individual joints and the average displacement (S_1) of the "intact" rock to the total shortening of the entire block. In terms of displacement: $D_2 = D_4 + D_6 + S_1$.

greater. In uniaxial compression the contribution of an individual joint (83%) is significantly greater than the contribution of the elastic deformation and the contribution of the microcracks (Figure 56). It is significant to note that the joints stiffened above 300 psi and the contribution of the joint was incrementally smaller. The deformation modulus of the block at low stresses (< 200 psi) was $.11 \times 10^6$ psi and 1.2×10^6 psi at higher stresses (2000 psi) indicating that both the joints and microcracks were closing. This modulus is still approximately a factor of 3 lower than the Young's modulus of 3.4×10^6 psi of small, intact specimens tested in the laboratory. The ultimate strength of this rock was 19,000 psi.

The factor by which the modulus of a small, intact specimen should be reduced is, therefore, dependent on the stress level of interest. At very low stresses (< 200 psi) the factor may range from 5 to perhaps as high as 30 depending on joint aperture and filling material. At higher stresses the reduction factor will be significantly lower approaching unity at high stresses. The compressional behavior (normal stiffness) of a joint at constant shear stress can be modelled by a function like the curve shown in Figure 57a.³⁶

The modulus ratio ($E_D/D_{T_{50}}$), relating the deformation modulus (E_D) obtained in the field to the modulus obtained in the laboratory ($E_{T_{50}}$) was found to be a correlative with spacing and character of joints as measured by rock quality (RQD) (Figure 58a) the ratio of seismic velocities obtained in the laboratory and in the field (V_F/V_L) (Figure 58b). The RQD or the velocity ratio along with laboratory values of modulus have been used to estimate the *in situ* deformation modulus. The correlation between these parameters is only fair, as indicated by the rather low correlation coefficients.

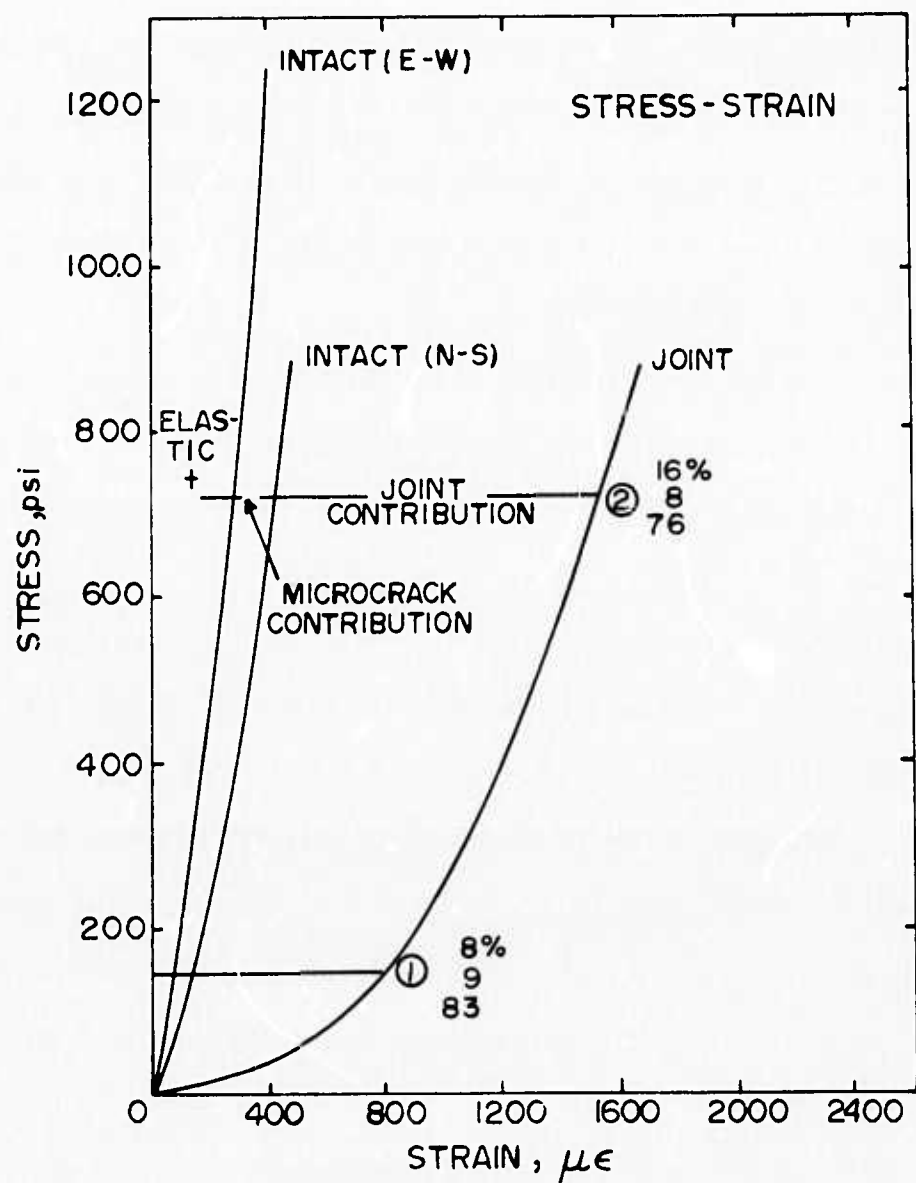


Figure 56. Comparative stress-strain curves showing the relative contributions of elastic, microfracture and joint deformation.

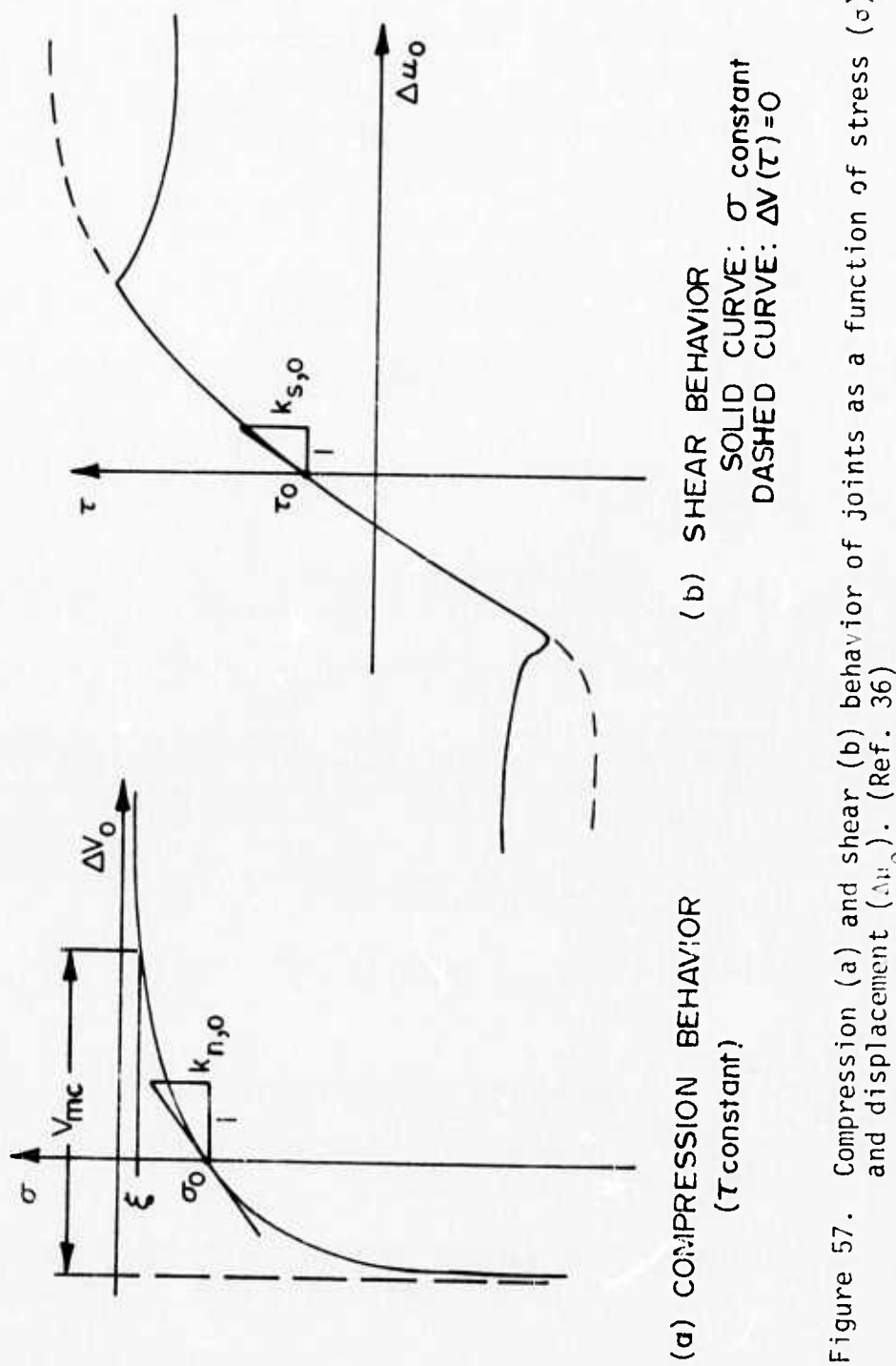
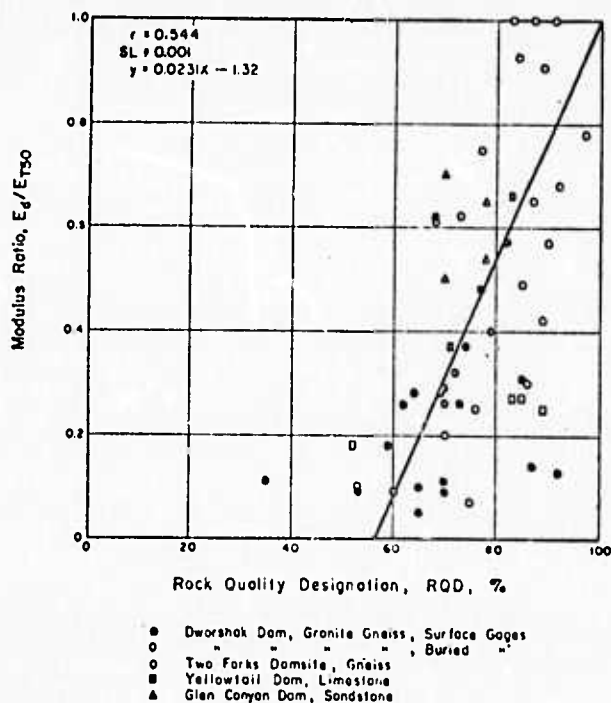
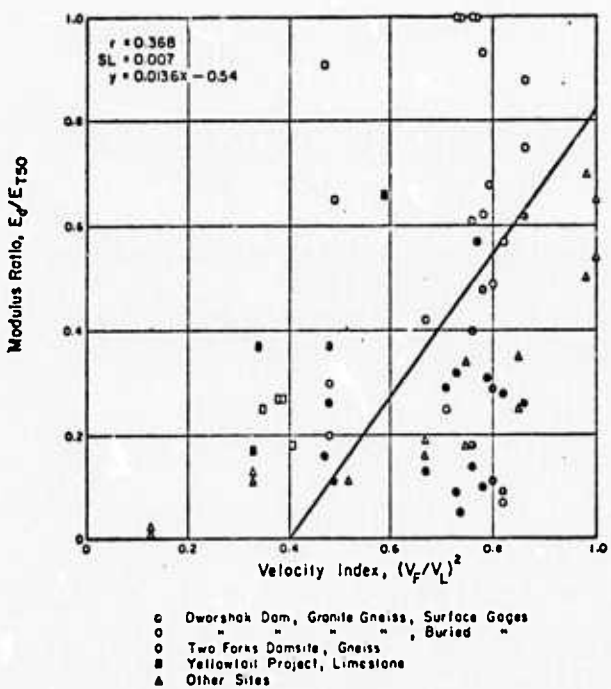


Figure 57. Compression (a) and shear (b) behavior of joints as a function of stress (σ) and displacement (Δu). (Ref. 36)



(a)



(b)

Figure 58. Variation of modulus ratio with RQD (a) velocity ratio (b).
(Ref. 24)

Experimental studies on rock and modeling material¹⁰ indicate that both the frictional strength and the stiffness of jointed media is a function of both the number and orientation of the joints (Figure 59). The failure envelope of the jointed material approaches that of intact material as the number of joints decrease with respect to the loading area and as the orientation becomes unfavorable for frictional sliding and as no block interaction enhances the strength or stiffness. Under high confining pressure the strength of jointed or fractured rock approaches that of intact rock.³⁷

The ultimate failure of intact rock has been shown to be independent of load path.³⁸ To date, the effect of load path on the frictional strength of jointed rock has not been studied. Direct and proportional shear tests on natural joints and sawcuts indicates that the frictional strength is sensitive to load path (Figures 48 and 49). Direct shear tests give a significantly higher friction angle than proportional shear tests on natural joints. A difference of 7 degrees was noted between the direct shear test and proportional shear tests along 30° and 37½° load paths. The difference may be due to the fact that asperities in the direct shear are interlocked by the applied normal load and it required a higher shear stress to cause sliding than in tests in which the shear and normal stresses are applied in a ratio in which the shear stress dominates. This reasoning is reinforced by the fact that a more pronounced difference in friction angle is seen in natural joints (7°) than for saw-cut surfaces (1°). Most structures (dams, silos, etc.) are, in reality, loaded in proportional shear rather than direct shear since both the normal and shear load

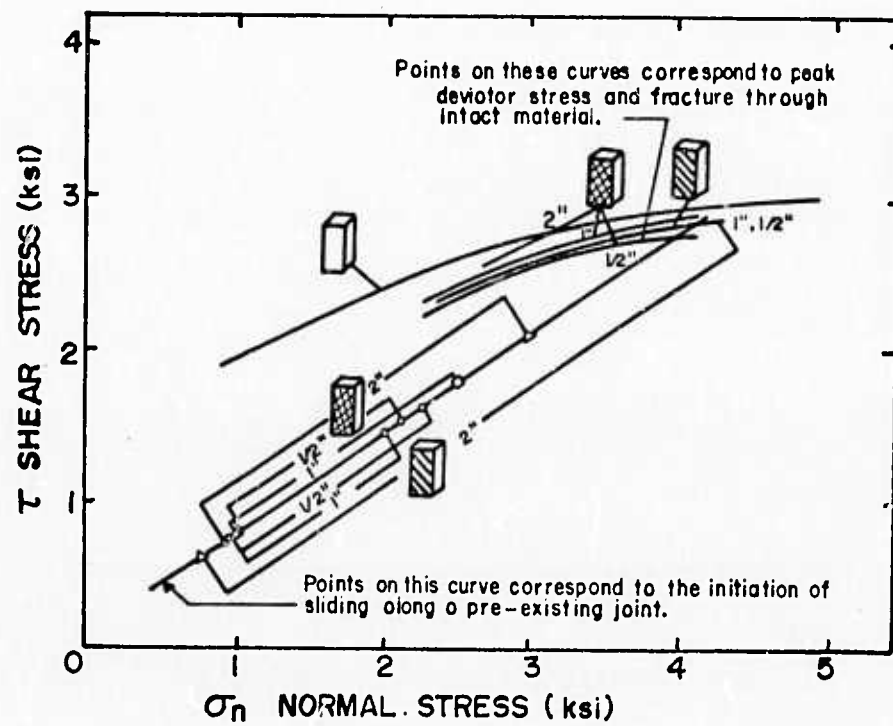


Figure 59. Failure envelopes for intact and jointed modeling material (after 10).

are applied simultaneously. The proportional load path would also be followed for the loading of joints at the edges of underground openings. The exact load path would depend on the orientation of the *in situ* joint or fracture sets with respect to the applied static or dynamic load.

The shear stiffness for a given normal stress also decreases with increasing specimen dimensions (Figure 60). The trends in our data agree with that presented by Barton⁷ on laboratory and *in situ* tests and data derived from model experiments. Because stiffness is a function of normal stress (Figure 61) at least up to a certain normal stress level, size effects must be couched in terms of given normal stress. The shear stiffness varies with displacement and is a function of the boundary conditions once the maximum shear stress has been obtained (Figure 57b).³⁶ This type of shear stiffness displacement relationship can be used for modelling shear behavior of a joint over a range of stress. The measured shear stiffness for large *in situ* samples has been as low as 500 psi/in.³² and as high as 50,000 psi/in. for prepared surfaces tested in the laboratory. The variation in shear stiffness values will have an impact on the results of any calculation of the response of a jointed rock mass.

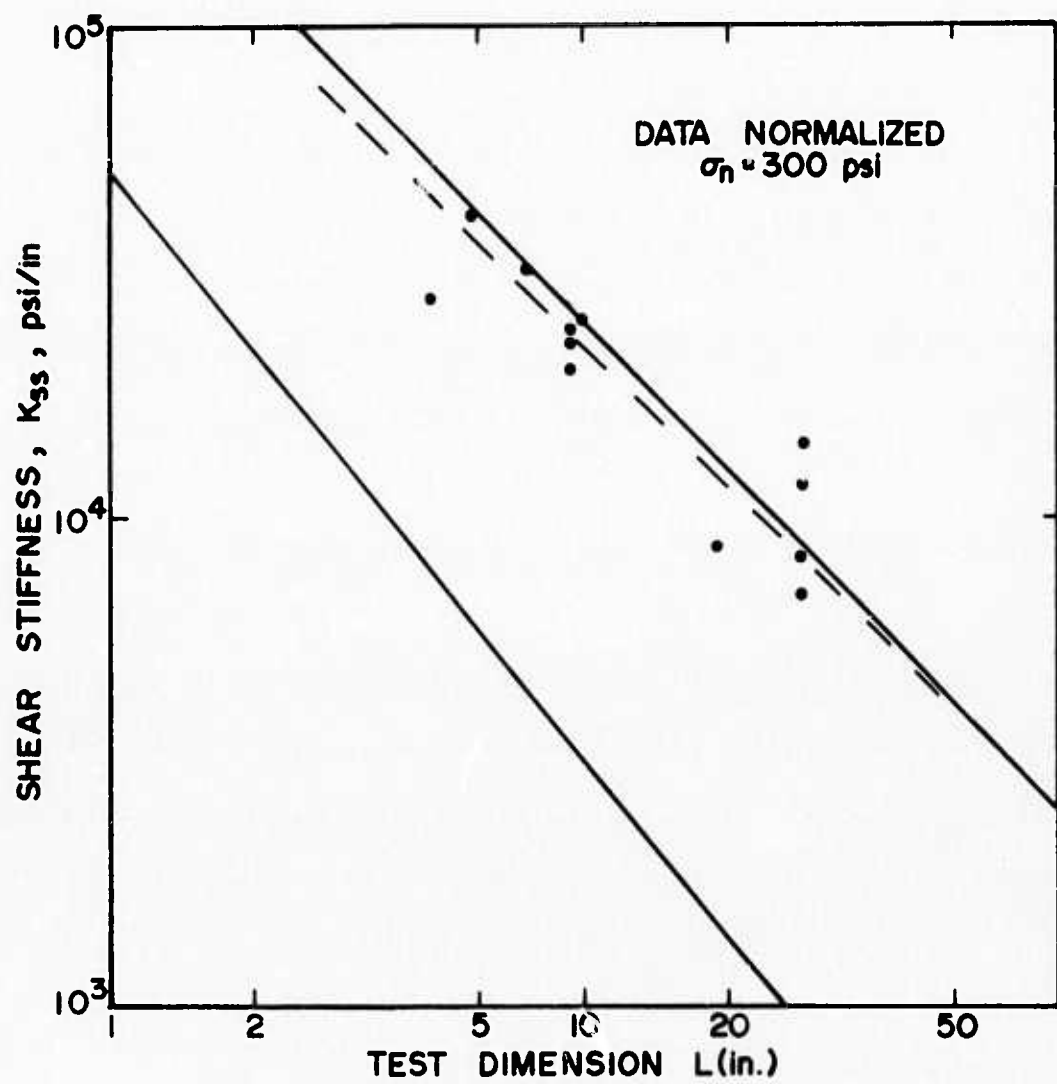
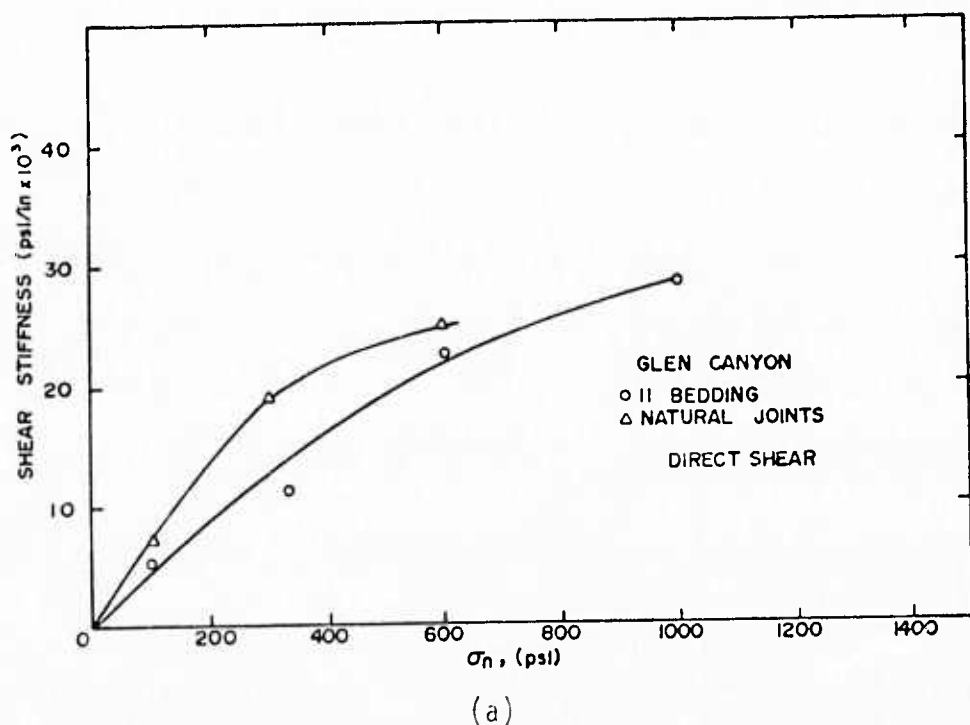
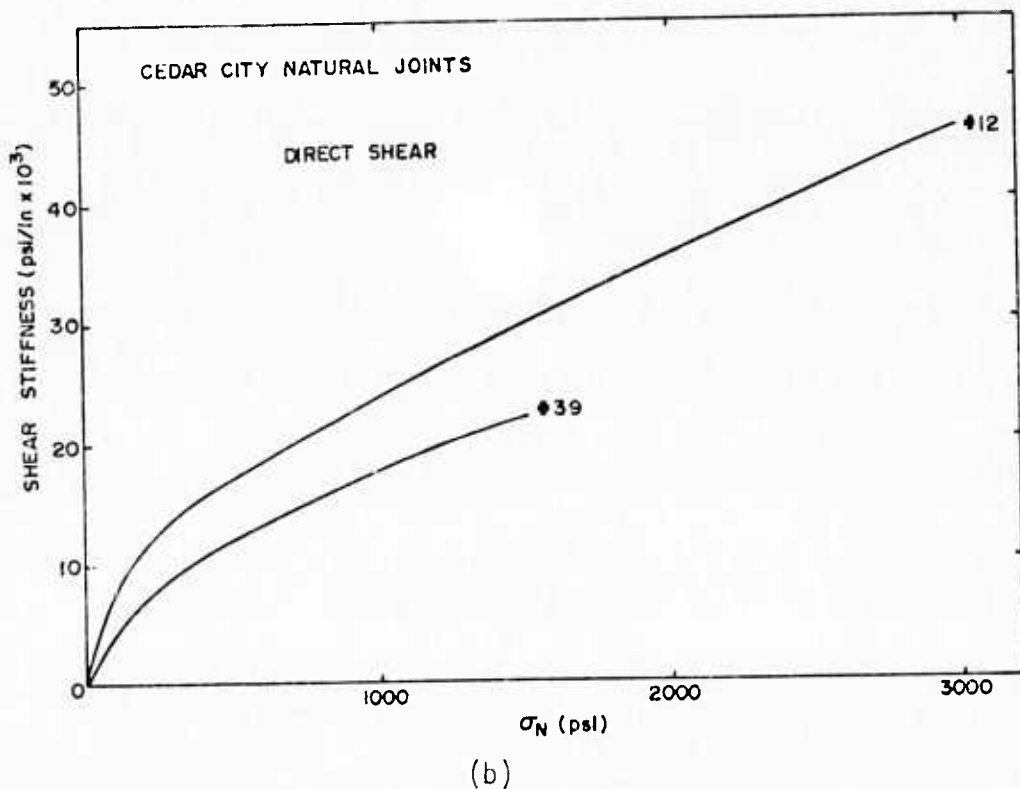


Figure 60. Shear stiffness as a function of joint surface area.
Dashed line represents range of other published data
(Ref. 7)



(a)



(b)

Figure 61. Shear stiffness as a function of normal stress for (a) sandstone and (b) diorite.

SECTION VIII

CONCLUSIONS

1. The testing technique developed by Terra Tek has advantages which make it a valuable tool for measuring the strength, deformation and frictional properties of *in situ* rock. The technique has been proven for a variety of rock types under a variety of field conditions ranging from flat outcrops to vertical walls in exploratory adits.
2. The strength and deformation modulus of *in situ* jointed rock may be up to a factor of 10 lower than the same properties obtained from small intact specimens. Constitutive relations developed for calculation of the response of large volumes of *in situ* rock must take into account these lower values.
3. Size effect curves must be established for both the strength and deformation of intact and jointed rock. Once the size effect for a particular rock has been found, then the strength and deformation of the rock can be estimated from laboratory values and scaled appropriately depending on the orientation and frequency of discontinuities.
4. The frictional properties of rock are load path dependent. Proportional shear tests of natural, undisturbed rock along load paths estimated from the orientation of joint sets in the field with respect to the applied load offer a viable method for measuring frictional strength and stiffness.

5. The Kayenta sandstone from the Mixed Company site exhibited a size effect of about a factor of 2. The mode of failure was along relict bedding planes. The rock also exhibited a marked anisotropy, even for small samples, which should be taken into account when modelling the site for dynamic calculations.

REFERENCES

1. Wallace, G. B., Searfim, E. J. and Anderson, F. A., "Foundation Testing for Auburn Dam," Proceedings of the Eleventh Symposium on Rock Mechanics, University of California, Berkeley. 1970.
2. Pratt, H. R., Black, A. D., Brown, W. and Brace, W. F., "The Effect of Specimen Size on the Mechanical Properties of Unjointed Diorite," *Int. J. Rock Mech. Min. Sci.*, 9, pp. 513-530. 1972.
3. Goodman, R. E., "The Deformability of Joints," *Proc. Am. Soc. Test. Mat.*, STP 477, pp. 174-196. 1970.
4. Patton, F. D., "Multiple Modes of Shear Failure in Rock and Related Materials," Ph.D. Thesis, University of Illinois. 1966.
5. Isenberg, J., "Nuclear Geophysics. Part II; Mechanical Properties of Earth Materials," Defense Nuclear Agency 1285H2, pp. 15-47. 1972.
6. Jaeger, J. C. and Cook, N. G. W., "Fundamentals of Rock Mechanics," Methuen, pp. 136-183. 1969.
7. Barton, N. R., "A Model Study of Rock-Joint Deformation," *Int. J. Rock Mech. Min. Sci.*, 9, 5. 1972.
8. John, K. W., "Engineering Methods to Determine Strength and Deformability of Regularly Jointed Rock," Proceedings of the Eleventh Symposium on Rock Mechanics, University of California, Berkeley. 1970.
9. Rosenblad, J. L., "Failure Modes of Jointed Rock Masses," Proceedings of the Second Congress, ISRM, Belgrade 2, pp. 3-42. 1970.
10. Einstein, H. and Hirschfeld, R. C., "Model Studies on Mechanics of Jointed Rock," *J. Soil Mech. Found. Div.*, 99, pp. 229-248. 1973.
11. Green, S. J. and Swanson, S. R., "Static Constitutive Relations for Concrete," Air Force Weapons Laboratory Technical Report AFWL-TR-72-244. 1973.
12. Schuster, S. H. and Isenberg, J., "Free Field Ground Motion for Beneficial Siting. Volume 2: Equation of State for Geologic Media," SAMS0-TR-70-88. 1970.

13. Nelson, I., et al., "Mathematical Models for Geological Materials for Wave Propagation Studies," DASA 2672, Paul Weidlinger Consulting Engineer. 1971.
14. DiMaggio, F. L. and Sandler, I., "Material Models for Soils," DASA-2521, Paul Weidlinger Consulting Engineer. 1970.
15. Herrmann, W. and Nunziato, J. W., "Nonlinear Constitutive Equations," Sandia Corporation SC-DC-72-1248. 1972.
16. Morland, L. W., "A Simple Continuum Model of Regularly Jointed Media," *Trans. Am. Geophys. Union*, 53, 11, p. 1118. 1972.
17. Singh, B., "Continuum Characterization of Jointed Rock Masses," *Int. J. Rock Mech. Min. Sci.*, 10, pp. 311-349. 1973.
18. Christiansen, L. M., Misterek, D. L. and Bowles, G. F., "Foundation Analysis of Auburn Damsite," Symposium of the International Society of Rock Mechanics, Nancy. 1971.
19. Goodman, R. E., Taylor, R. L. and Brekke, T. L. A., "A Model for the Mechanics of Jointed Rock," Proceedings of the American Society of Civil Engineers, SM# 94, pp. 637-659. 1968.
20. Mahtab, M. A. and Goodman, R. E., "Three-Dimensional Finite Element Analysis of Jointed Rock Slopes," Proceedings of the Second International Congress, Belgrade, 3. 1970.
21. Cundall, P. A., "A Computer Model for Simulating Progressive Large-Scale Movements in Blocky Rock Systems," Proceedings of the International Symposium, ISRM, Nancy. 1971.
22. VonThon, J. L. and Tarbox, G. S., "Deformation Moduli Determined by Joint-Shear Index and Shear Catalog," Proceedings of the International Symposium, ISRM, Nancy. 1971.
23. Bellport, B. P., "Morrow Point Dam and Powerplant Foundation Investigation," U.S. Bureau of Reclamation. October 1965.
24. Coon, R. F. and Merritt, A. H., "Predicting *In Situ* Modulus of Deformation Using Rock Quality Indexes," *Am. Soc. Test. Mat.*, STP 477, pp. 154-173. 1970.
25. Brown, E. T., "Strength - Size Effects in Rock Material," Mineral Resources Research Center, Project Report 24, University of Minnesota, pp. 138-150. 1971.
26. Hodgson, K. and Cook, N.G.W., "The Effects of Size and Stress Gradient on the Strength of Rock," Proceedings of the Second International Conference of Rock Mechanics, Belgrad, 2, pp. 3-5. 1970.

27. Mogi, K., "The Influence of the Dimensions of Specimens on the Fracture Strength of Rocks," *Bull. Earthquake Res. Inst.*, 40, pp. 175-185. 1962.
28. Bieniawski, Z. T., "Propagation of Brittle Fracture in Rock," CSIR Report MEG 664, Pretoria South Africa, Presented at Tenth Symposium on Rock Mechanics, Austin, Texas. 1968.
29. Huck, P. J., "Effect of Specimen Size on Confined Compression Testing of Rock Cores," IITRI Project No. D6059. 1972.
30. Bieniawski, Z. T., "The Effect of Specimen Size on the Compressive Strength of Coal," *Int. J. Rock Mech. Min. Sci.*, 5, p. 325. 1968.
31. Scholz, C., "Experimental Study of the Fracturing Process in Brittle Rock," *J. Geophys. Res.*, 73, pp. 1447-1454. 1968.
32. Evdokimov, P. D. and Sapegin, D. D., "A Large-Scale Field Shear Test on Rock," Proceedings of the Second International Congress on Rock Mechanics, Belgrade, pp. 3-17. 1970.
33. Pratt, H. R., Black, A. D. and Bonney, F. J., "Frictional Properties of Cedar City Quartz Diorite," Air Force Weapons Laboratory, AFWL TR-72-122. 1972.
34. Stowe, R. L., "Comparison of *In Situ* and Laboratory Test Results on Granite," *AIME Trans.*, 252, pp. 195-198. 1972.
35. Pratt, H. R., Swolfs, H. S. and Black, A. D., "Properties of *In Situ* Jointed Granite," Progress Report No. 4, Army Research Office and Terra Tek TR 74-18. 1974.
36. Goodman, R. (University of California). Personal communication, 1974.
37. Byerlee, J. D., "Frictional Characteristics of Granite Under High Confining Pressure," *J. Geophys. Res.*, 72, pp. 3639-3648. 1967.
38. Swanson, S. R. and Brown, W. S., "An Observation of Loading Path Independence of Fracture in Rock," *Int. J. Rock Mech. Min. Sci.*, 8, pp. 277-281. 1971.